UNIVERSITY OF CALIFORNIA, SAN DIEGO

Structure/Function Analysis of Ubiquitin C-terminal Hydrolase – L1 (UCH-L1)

A thesis submitted in partial satisfaction of the requirements for the degree

Master of Science

in

Biology

by

Afshin Salehi

Committee in charge:

Professor Gentry N. Patrick, Chair
Professor Nicholas Spitzer
Professor James Wilhelm

2009

This thesis of Afshin Salehi is approved and it is acceptable in quality and form from publication on microfilm and electronically:

_____

_____

_____
Chair

University of California, San Diego

2009

DEDICATION

This work is dedicated to my Mom, Dad, and sister for their continuous and tremendous love and support. Your enormous strength and encouragement empowers me as I face every journey in my life.

Thank you and I love you!

EPIGRAPH

Human beings are members of a whole,
In creation of one essence and soul.
If one member is afflicted with pain,
Other members uneasy will remain.
If you have no sympathy for human pain,
The name of human you cannot retain.

Persian poet **Sa'di of Shiraz**

TABLE OF CONTENTS

LIST OF ABBREVIATIONS

AD:	Alzheimer's disease
ALS:	Amyotrophic lateral sclerosis
APV	(2R)-amino-5-phosphonovaleric acid
DIV	Days in vitro
dsRNA	double stranded RNA
fUb	free ubiquitin
Gly	Glycine
HD:	Huntington's disease
LB	Lowy Body
LTD	long term depression
LTF	long term facilitation
LTP	long term potentiation
NMDA:	N-methyl-D-aspartic acid
PD:	Parkinson's disease
PSD	Post synaptic density
RT	room temperature
Syn	synapsin I
Ub	Ubiquitin
UPS	ubiquitin proteasome system

LIST OF FIGURES

ACKNOWLEDGEMENTS

I would like to greatly thank Dr. Gentry N. Patrick for welcoming me to his laboratory and allowing my growth in carrying out independent scientific research. He has encouraged my aspirations, and helped me in my research projects throughout the past two years, particularly in the past year. I would also like to thank Dr. Anna Cartier with whom I initially worked with and learned a great deal about basic molecular techniques in the Patrick lab.

Moreover, I would like to thank the members of the Patrick lab, Steven Djakovic, Lindsay Schwarz, and Jeffrey M. Keil who helped me throughout this journey. They not only helped me troubleshoot countless experiments gone awry, but also shared with me their kindness, wisdom, and friendship. In addition, I would like to show appreciation toward all the help that I received from Alan Okada. He not only helped me with experiments in lab but he also edited much of the writing in this thesis. Without his help, completion of my Masters degree would have taken much longer.

Most importantly, I would not have achieved my goals thus far had it not been for the encouragement, support, and the teachings of my

family. Their unconditional love, always available ears, strength, and knowledge have provided me with the ability to set my goals high and achieve them one by one. Thus, here is thank you to Mom, Zahra Ahmadi, Dad, Massoud Salehi, and my sister and best friend Mitra Salehi. Furthermore, I want to especially thank Shonda Letchworth for always being by my side, yet giving me the time and understanding I needed to complete this journey.

I also want to thank the following people for their friendship and support: Kenny Gros, Amir Motamedi, Roger (Eric) Xu.

Figures 2-9, is a reprint of Figures 2, 3, 8, and part of figure 7 as it appears in Anna E. Cartier, Steven N. Djakovic, Afshin Salehi, Scott M. Wilson, Eliezer Masliah, and Gentry N. Patrick, 2009 Regulation of Synaptic Structure by Ubiquitin C-Terminal Hydrolase L1. J Neurosci, 2009. 29(24): p. 7857-68. The author of the thesis was an author of this paper, and conducted some of the experiments resulting in those figures in collaboration with the other authors.

ABSTRACT OF THE THESIS

Structure/Function Analysis of Ubiquitin C-terminal Hydrolase – L1 (UCH-L1)

by

Afshin Salehi

Master of Science in Biology

University of California, San Diego, 2009

Professor Gentry N. Patrick, Chair

Parkinson's disease (PD) and Alzheimer's disease (AD), two of the most common neurodegenerative diseases, are caused by both genetic and environmental factors. Mammalian neuronal cells abundantly express a deubiquitinating (DUB) enzyme, Ubiquitin Carboxy-terminal hydrolase L1 (UCH-L1), which is involved in the pathogenesis of both of these neurodegenerative diseases. This DUB is selectively expressed in the brain

and its activity is required for normal synaptic function. Here we show that UCH-L1 activity is up-regulated by NMDA receptor activation and that this upregulation leads to increase in mono-Ub levels in the cell. Furthermore, we show that pharmacological inhibition of UCH-L1 leads to reduction of mono-Ub levels in the cell and causes dramatic alterations in size and distribution of many pre- and post- synaptic proteins. Moreover, for the first time we show that, both *in vitro* and *in vivo,* application of UCH-L1 specific inhibitor LDN, reduces UCH-L1 ability to bind to ubiquitin. In addition to using pharmacology, genetic tools such as RNAi against UCH-L1 and overexpression of mutant constructs were used to study the effect of altered UCH-L1 activity on synaptic protein composition. These findings suggest that through modulating mono-ubiquitin levels in cells, in an activity dependent manner, UCH-L1 plays an important role in neuronal synaptic remodeling.

INTRODUCTION

Ubiquitin Proteasome System

The ubiquitin proteasome system (UPS) is the major eukaryotic cellular pathway that controls protein turnover via the 26S proteasome. In eukaryotic cells many basic cellular processes such as cell cycle progression, signal transduction, apoptosis, trafficking, and protein quality control are regulated by the UPS (1-3). Induction of the process leading to proteasomal degradation is achieved through the tagging of targeted proteins with a small molecule known as ubiquitin. Ubiquitin is a highly conserved 76 amino acid protein that can be covalently linked to lysine residues on the targeted proteins in a process called ubiquitination.

Ubiquitination is a multi-step process that requires the activity of three classes of enzymes, an ubiquitin-activating enzyme (E1), an ubiquitin-conjugating enzyme (E2), and a specific ubiquitin-protein ligase (E3) (4). The ubiquitin-activating enzyme works in an ATP-dependent manner to attach its active-site cysteine residue to the C-terminal glycine residue of ubiquitin in a high-energy thioester linkage, thereby activating ubiquitin. The activated ubiquitin can then be transferred to E2 enzymes, of which there are relatively few found in eukaryotic cells, through a trans (thio) esterification reaction. Finally ubiquitin is attached to lysine residues

on the target protein with an isopeptide bond. This step requires the activity of one of the hundreds of E3 ubiquitin-protein ligase enzymes. E3s act as substrate recognition modules and are capable of interacting with both E2 and the protein substrates (5).

The E3 enzymes (also known as ubiquitin ligase proteins) possess one of two types of domains. One category has a zinc-binding RING (Really Interesting New Gene) finger domain which promotes ubiquitination by binding an E2 as well as a substrate (6). The other category has a HECT (Homologous to E6-AP Carboxy-terminus) domain which directly binds to ubiquitin and then transfers it to a substrate. In some cases the ubiquitination process stops at this stage which would leave the targeted protein monoubiquitinated. However, ubiquitination is often continued through the attachment of another free ubiquitin molecule to specific lysine residues in the last ubiquitin of the growing ubiquitin chain. In this fashion and with subsequent iterations of this process, a target protein can become polyubiquitinated. Some proteins require the action of an ubiquitin-chain elongation-factor, E4 to be able to be ubiquitinated efficiently (7).

Ubiquitin-chain linkage acts as a stamp for functionally distinct processes that are not only limited to proteasome degradation. Originally it was assumed that polyubiquitinated proteins are exclusively targeted to

the 26S proteasome. However, it is now know that ubiquitin signaling is much more versatile (8). Polyubiquitination can occur in one of two forms, homo- or hetero-polymeric. In the homopolymeric form, ubiquitin molecules are attached to each other using the same donor lysine residue. Homopolymeric ubiquitin chains have been found to extend through linkages from several lysine residues found on the ubiquitin molecule: Lys^{48}, Lys^{63}, Lys^{6}, Lys^{11}, Lys^{29}, Lys^{27} and Lys^{33}. Each of these types of linkages results in a specific signaling cascade. For example addition of a Lys^{48} linked chain to a protein functions as a degradation signal while Lys^{63} can be a signal for DNA repair, endocytosis or signal transduction. Heteropolymeric polyubiquitin chains are characterized by conjugation of ubiquitin molecules through more than one type of linkage (7). The properties of heteropolymeric chains are not well studied.

Deubiquitinating enzymes (DUBs)

Ubiquitination is a reversible process. Similar to the activity of phosphatases that can remove phosphate groups from phosphorylated proteins, there is a group of enzymes that can remove the ubiquitin moiety from ubiquitinated proteins. These proteins are called deubiquitinating enzymes (DUBs). DUBs are cysteine proteases that can

hydrolyze the isopeptide bond between the ubiquitin and its substrate by ATP-dependent hydrolysis (9). Much the same as ubiquitination, deubiquitination is a very much controlled process which has been linked to cell cycle regulation (10), gene expression (11), proteasome-and-lysosome-dependent protein degradation (12-14), DNA repair (15), kinase activation (13) and many more cellular functions. DUBs play several roles in the ubiquitin pathway. First, DUBs can antagonize the ubiquitination process by removing ubiquitin from the ubiquitinated proteins in a cell (16-17). Seconds, DUBs participate in activating ubiquitin proproteins. Ubiquitin is always expressed either as a proprotein that is attached to ribosomal proteins, or it is expressed as a linear polyubiquitin chain that needs to be hydrolyzed to single ubiquitin molecules (18-19). Third, DUBs recycle the ubiquitin that has been trapped by thiol ester bonds between ubiquitin and small cellular nucleophiles (20). Finally, DUBs generate free monomeric ubiquitin from unanchored polyubiquitin chains within cells (21-22). This population includes free polyubiquitin that is made by conjugating enzymes or ubiquitin that has been released in polyubiquitin from other deubiquitinated proteins.

In Eukaryotic cells DUBs are subdivided into five families based on their structures and functions. These families are ubiquitin-specific proteases (USPs), ubiquitin C-terminal hydrolases (UCHs), Otubain

proteases (OTUs), Machado-Joseph disease proteases (MJDs) and a subset of metalloproteases (17). In most cases DUB activity is cryptic (23). That is, energy is required for the DUB to associate with its substrate and achieve a catalytically competent conformation. The cryptic nature of DUB function provides a mechanism for regulating the DUB's level of activity in a cell, which in turn helps to prevent inappropriate degradation of proteins. Other means by which DUBs are regulated includes phosphorylation, ubiquitination, and sumoylation.

Ubiquitin Proteasome System Function in Neurons

The UPS has emerged as a key protein modification and degradation pathway that is crucial for the development, maintenance and remodeling of synaptic connections in the brain (24-25). Given the wide range of cellular pathways and physiological processes in which ubiquitin is involved; it is not surprising that normal neuronal function depends largely on an intact UPS system. For example synaptic connections are established in a highly regulated fashion during development. It is thought that initially there are many more synapses formed than the final number retained in the fully developed nervous system and this process has been shown to be mediated, in part, by UPS

activity (26). Additionally, the UPS is involved in dendritic pruning in the *Drosophila* nervous system. Pruning is a process that occurs during metamorphosis in *Drosophila*. During metamorphosis a group of sensory neurons called the class IV dendritic arborization (C4da) go through complete pruning of their larval dendrites to re-grow a new dendritic network. In 2006, a group at UCSF was able to show that pruning was associated with the activity of specific E2/E3 enzymes (25). Among other functions regulated by the UPS, studies have showed that the UPS is involved in controlling the number of synapses in a neuron (27-28). Overexpression of a DUB called 'fat facets' and loss of function of an E3 called 'high wire' has been shown to cause an increase in synaptic branching and the number of synaptic boutons in the neuromuscular junction (29). In the same study, Ashok and colleagues also demonstrated that synaptic size is regulated by the UPS (29).

It has been well-documented that modifications in synaptic efficacy are accompanied by a change in the protein composition of synapses (30). A change in the protein composition of synapses can arise by the incorporation of newly synthesized proteins or by the selective destabilization and removal of existing proteins. Aspects of this simultaneous and dynamic interplay between the production and degradation of key synaptic components, as well as the concomitant

effects on the efficacy of synaptic transmission seem to be highly regulated by the UPS. One of the early UPS involvements in synaptic regulation was the discovery that the Regulatory (R) subunits of Protein Kinase A (PKA) were found to be decreased during induction of long-term facilitation (LTF), a form of synaptic plasticity, in *Aplysia.* Importantly, it was found that this decrease was due to the ubiquitination and proteasome-mediated degradation of the R subunits of PKA (31).

Furthermore, ongoing or activity-dependent protein degradation is suggested to be required for neuronal plasticity in the mammalian hippocampus by the fact that proteasome inhibition can attenuate long term potentiation (LTP) and long term depression (LTD), both of which are forms of synaptic plasticity involved in learning and memory in the hippocampus. Proteasome inhibition was found to block NMDA-dependant and mGluR-dependent synaptic depression (32-34). Interestingly, there appears to be a strict balance between new protein synthesis and protein degradation via the proteasome. Evident by the finding that while the application of protein synthesis inhibitors or proteasome inhibitors alone can block LTP, simultaneous application of both of these drugs has an occlusive effect and will leave LTP unaltered (35).

Moreover, serotonin (5-HT), which induces LTF in Aplysia, has been shown to encourage the interaction of a DUB called Ap-uch with the proteasome. As will be discussed in greater detail later, the mammalian homolog of Ap-uch, ubiquitin C-terminal hydrolase L1 (UCH-L1), has also been reported to play a role in contextual fear learning and LTP (36). All of these studies, when taken together, highlight the fact that UPS-mediated regulation of neuronal protein composition and quality is critical in maintaining the normal physiological function of neurons as well as participating in activity-dependent plasticity events such as learning and memory.

Neurodegenerative disease and UPS

The UPS has been linked to many diseases of the nervous system. Alzheimer's disease (AD)(37) and other clinically distinct neurodegenerative disorders such as Parkinson's disease (PD)(38), Amyotrophic Lateral Sclerosis (ALS) and Huntington's disease (HD)(39) all share common neuropathological features. Collectively, these diseases are now considered 'proteinopathies' of the nervous system, characterized by accumulation of misfolded protein aggregates that are resistant to degradation. Ubiquitinated proteins are found in these

pathological aggregates, which include plaques and tangles (AD), Lewy bodies (PD), and plyQ inclusion bodies (HD) (40-42) This is suggestive of the possibility that proteins in the aggregates are marked for degradation but are not efficiently removed (42). In Dementia with Lewy bodies (DLB) and PD patients, it was found that the ubiquitin chain length on a-synuclein was between one and three ubiquitins (43), which raises the possibility that it is inefficiently targeted to the proteasome as ubiquitin chain lengths of four or more are required for recognition and degradation by the proteasome. Proteasome activity is substantially decreased in AD and PD (44). Therefore, it is possible that UPS dysfunction may be due to an increased load of misfolded proteins and protein aggregates and the inability to recognize and degrade them.

A considerable portion of our current understanding about UPS dysfunction in neurodegenerative disease has come from the identification of genes linked to familial and sporadic forms of PD. Ten genetic loci responsible for rare Mendelian forms of PD have been identified by linkage analysis. Of the genes cloned, two are components of the UPS. First, the *PARK2* gene encodes an E2-dependent E3 ligase, parkin(45-46). *PARK2* mutations appear to be loss-of-function mutations (45) and lead to early onset PD, with loss of dopaminergic neurons in the Substantia Nigra in the absence of Lewy Bodies (47). This strongly suggests

that UPS dysfunction contributes to PD pathogenesis. Another cloned gene, *PARK5*, which encodes for UCH-L1, a DUB that has both hydrolase and ligase functionality (48-49), has been associated with familial and sporadic PD (38, 50) in humans. A spontaneous mutation in UCH-L1 found in gracile axonal dystrophy (*gad*) mice exhibit retrograde accumulation of β-amyloid aggregates but not α-synuclein aggregates in the gracile tract axons (51-52). Since UCH-L1 is thought to help maintain monomeric ubiquitin levels in neurons, the deposition of aggregate-prone proteins could be a secondary effect(53).

Ubiquitin carboxy-terminal hydrolase L1 (UCH-L1) function and its relation to neurodegenerative disease

Ubiquitin C-terminal hydrolase L1 (UCH-L1), also known as PGP9.5, is a protein of 223 amino acids (54) and an important component of the UPS. It belongs to a family of DUBs comprised of UCH-L1 – UCH-L5. UCH-L1 is selectively and abundantly expressed in neurons, representing 1-2% of total soluble protein in the brain (54). Although originally it was thought that UCH-L1 functioned solely as a deubiquitinating enzyme (54), more recent studies have suggested that it may carry out a greater role within the UPS. UCH-L1 is known to generate free monomeric ubiquitin from

either precursor ubiquitin poly-peptides or from ubiquitin fused to small ribosomal proteins (55-56). Recent *in vitro* studies also show that UCH-L1 possesses ubiquitin ligase ability (48). In addition to its enzymatic capabilities UCH-L1 associates with ubiquitin to inhibit its lysosomal degradation and, therefore, can maintain and stabilize monomeric ubiquitin levels in neurons (49).

Many studies have demonstrated a link between UCH-L1 and neurodegenerative disorders such as AD and PD. The implications supporting a role for UCH-L1 dysfunction in PD were initially based on the discovery of a mutation found in the UCH-L1 gene carried by two siblings in a German family with autosomal dominant PD (57). In this mutation the isoleucine at position 93 has been changed into a methionine and the gene product is thus termed UCH-L1 I93M. Only one of the two UCH-L1 alleles is altered in the I93M mutation carried within this family, indicating that it is autosomal dominant in nature. However, the parents of the affected siblings are unaffected which may suggest that the I93M mutation may be a rare polymorphism that can segregate with disease, or that the mutation displays incomplete penetrance (48). Functionally, this mutation leads to a 50% reduction in the catalytic activity of the protein *in vitro*. Therefore, it is implied that that the loss of UCH-L1 function may reduce the availability of free ubiquitin, and contribute to an

impaired clearance of proteins by the UPS. Furthermore, transgenic mice that express the I93M mutation exhibit a significant reduction in dopaminergic neurons in the substantia nigra, and the dopamine content in the striatum (58).

As was mentioned earlier, UCH-L1 is believed to possess ubiquitin ligase activity. *In vitro* experiments with UCH-L1 have shown this ligase ability is dimerization-dependent and is responsible for the ubiquitination of α-synuclein, possibly with a K63 chain link. α-synuclein is a protein enriched in pre-synaptic terminals, and is involved in neurotransmitter release (59). This protein is a major component of pathogenic insoluble proteinaceous deposits known as Lewy bodies (LBs) which are commonly found in PD brains. A recent report demonstrated that UCH-L1 is localized to synaptic vesicles and co-immunoprecipitates with α-synuclein from rat brains (48). It is believed that the ubiquitination of α-synuclein on K63 by UCH-L1 blocks its proteasomal degradation and leads to its accumulation and aggregation within neurons and Lewy bodies (48). Normally α-synuclein exists in a monomeric state, but when a high concentration of α-synuclein is present it can polymerize into filaments which leads to its eventual precipitation within the proteinaceous inclusions characteristic of LBs. Interestingly, there is another naturally occurring UCH-L1 polymorphism that has been shown to have reduced ligase ability. This mutation has

been found throughout certain populations within East Asia and is characterized by a change of serine 18 to a tyrosine and is thusly referred to as UCH-L1 S18Y. The S18Y mutation of UCH-L1 leads to reduced levels of ubiquitinated α-synuclein and is associated with a lowered risk of developing PD.

UCH-L1 is required for the maintenance of LTP in neurons. A very convincing study to come out of the lab of Ottavio Arancio's in 2006 demonstrated this requirement of UCH-L1 for synaptic plasticity in mice lacking UCH-L1 (36). These mice, termed gracile axonal dystrophy (*gad)* mice have a naturally occurring in-frame deletion of exons 7 and 8 in the Uch-l1 gene. Expression of the UCH-L1 protein is undetectable in the central nervous system of these mice (49). *Gad* mice exhibit motor paresis due to axonal degeneration of spinal cord neurons and subsequent degeneration of the spinocerebellar tract. Data from these studies, using UCH-L1 lacking mice, demonstrated that despite the absence of any gross structural abnormalities in the brains of these mice, UCH-L1 is required for the maintenance of contextual memory and transcription-dependent LTP induced by theta-burst stimulation in the CA1 area of the hippocampus (36). Interestingly, *gad* mice also exhibited reduced levels of monomeric ubiquitin levels in neurons, which may suggest that ubiquitin homeostasis could also play a role in learning and memory.

Taken together all these studies are elusive to the fact that UCH-L1 seems to be highly involved in normal neuronal physiology, learning, memory, and its dysfunction can contribute to neurodegenerative diseases.

Significance behind studying UCH-L1

As it was mentioned earlier, UCH-L1 dysfunction has been shown to be associated with a number of neurodegenerative diseases like AD and PD. This DUB is commonly found in the neurofibrillary tangles observed in AD brains (60). Gong et. al. performed a convincing study where they demonstrated that transduction of the UCH-L1 protein into the hippocampi of APP/PS1 mice, a commonly used mouse model of AD, can restore both the synaptic and cognitive defects observed in these mice (36). In addition, another finding emphasizing the link between UCH-L1 and neurodegenerative diseases reported UCH-L1 to be down regulated in AD and idiopathic PD and that this protein is a major target of oxidative damage (60). Furthermore, synaptic damage and loss are considered to be key factors of the cognitive defects observed in neurodegenerative diseases. Taken together these data suggest the possibility that UCH-L1 function may be required for maintaining normal synaptic structure and

function. More specifically, UCH-L1 dysfunction and loss, observed in neurodegenerative diseases, could be somehow related to the damage and alteration of synaptic structure and thereby cognitive and learning defects.

The impetus behind studying the role of UCH-L1 on hippocampal synaptic spines was a consequence of a novel finding by Dr. Anna Cartier in our lab. As it will be discussed in greater detail in the following text, we have uncovered a novel interplay between neuronal activity, stimulated by NMDA application, UCH-L1 function and monomeric ubiquitin levels(61). Furthermore, altered activity of UCH-L1 through pharmacological inhibition, had drastic effects on the synaptic protein clusters and dendritic spine size and density(61).

Given the afore mentioned finding, we hypothesized that UCH-L1plays an important role in the maintenance of synaptic structure perhaps by means of its main function which is modulating free monomeric ubiquitin levels in neurons. Therefore to follow up and validate Cartier's finding and to define how UCH-L1 function affects synaptic structure I took several approaches to alter UCH-L1 function in cultured hippocampal neurons. Pharmacological inhibition, RNAi mediated knockdown and over expression strategies are being used to manipulate various activities of UCH-L1. These altered conditions are then compared

to control neurons to characterize the spines and synapses for morphological changes. Furthermore, using biochemistry I am searching for additional proteins that may be interacting with UCH-L1 within hippocampal neurons in order to better understand the molecular mechanisms underlying the structural and functional abnormalities we have uncovered through the various genetic manipulations I have utilized.

MATERIALS AND METHOD

Reagents

UCH-L1 (LDN-57444 (LDN)) was purchased from Calbiochem. NMDA and D(-)-2-amino-5-phosphonopentanoic acid (APV) (NMDA receptor antagonist) were purchased from Tocris Bioscience (Bristol, United Kingdom). The hemagglutinin (HA)-tagged ubiquitin probe (HAUb-VME; vinyl methyl ester functionalized probe) was synthesized as described previously (Borodovsky et al., 2002) and was provided by Dr. H. Ovaa (The Netherlands Cancer Institute, Amsterdam, The Netherlands).

Antibodies

The following antibodies were used in this study: rabbit and mouse anti UCH-L1 (BIOMOL); rabbit anti-ubiquitin (Dako); mouse anti-Myc; mouse anti-postsynaptic density-95 (PSD95) (obtained from Calbiochem); rabbit anti-shank antibody (a generous gift from Dr. Eunjoon Kim, Korea Advanced Institute of Science and Technology, Daejeonm Korea); rabbit anti-synapsin I (Millpore Bioscience Research Reagents); and mouse anti-HA

Primary neuronal cultures

Hippocampal neuron cultures were prepared from postnatal day 1 (P1) or P2 rat hippocampi as previously described (Patrick et al., 2003). Briefly, for immunostaining experiments, rat hippocampi were dissected, dissociated by papain treatment and mechanical trituration, and plated at medium density (45,000 cells/cm 2) on poly-D-lysine-coated coverslips (12 mm in diameter) or glass-bottom dishes (MatTek; 35 mm). For the purpose of biochemical experiments, mixed hippocampal and cortical neurons were plated at high density on six-well plates (~500,000 cells per well) coated with poly-D-lysine. Cultures were maintained in B27 supplemented Neurobasal media (Invitrogen) until 14–21 d *in vitro* (DIV).

Recombinant DNA and Sindbis constructs

The Sindbis enhanced green fluorescent protein (EGFP) viral construct was made by cloning the EGFP (Clontech) open reading frame directly into pSinRep5 (Invitrogen). For production of recombinant Sindbis virions, RNA was transcribed using the SP6 mMessage mMachine Kit (Ambion) and electroporated into BHK cells using a BTX ECM 600 at 220 V, 129Ω, and 1050 μF. Virions were collected after 24–32 h and stored at -80°C until use. For UCH-L1expression constructs, the UCH-L1 open reading

frame was obtained from Incyte full-length human cDNA clone (Open Biosystems) encoding wild-type UCH-L1 and was amplified by PCR with a 5'-oligo containing a *Xho*I site and a 3'-oligo containing an *Age*I site, and subsequently cloned in the pEGFP-N1 vector. The single point mutations in the UCH-L1 DNA were introduced by PCR-based site-directed mutagenesis of template plasmid cDNA using primers designed to introduce specific mutations (C90S, 5'-CCATTGGGAATTCCTCTGGCATCGGAC-3', and D30A, 5'-TTCGTGGCCCTGGGGCTG-3'). All constructs were verified by sequencing and by expression of proteins of the expected molecular weight in HEK 293T cells.

Fractionations and DUB labeling assay

Fractions from rat brains were prepared as previously described in (62-63). The DUB activity assay was done by incubating 20 µg of lysates from neuronal cultures or rat brain fractions with the HAUb-VME substrate in labeling buffer (50 mM Tris, pH 7.4, 5 mM $MgCl_2$, 250 mM sucrose, 1 mM DTT, and 1 mM ATP) for 1 h at 37°C. Proteins were then resolved on SDS-PAGE 4-20% gradient gels, and blots were subsequently probed with anti-HA monoclonal antibody. Labeled proteins were identified based on their

migration on SDS-PAGE gels, and by comparison to previous published data where the specific bands were analyzed by mass spectroscopy (64)

Drug treatments and virus infections

For protein expression analysis by Western blotting or immunofluorescence staining experiments, cultured neurons were treated with 10 μM UCH-L1 (LDN) or UCH-L3 inhibitor for 24 h. In experiments in which neurons were subjected to LDN treatment and infections, neurons were first treated with LDN and then infected by adding virions directly to the culture medium and allowing protein expression for 12–14 h. The total time of exposure to LDN was kept constant (24 h). Activity stimulation experiments were performed by treating cultures with NMDA and glycine at 50 and 10 μM, respectively, for 10 min at 37°C. Where indicated, neurons were pretreated with UCH-L1 inhibitor (10 μM) for 24 h or APV (50 μM) for 10 min before addition of NMDA/glycine to the culture media.

Immunostaining

At the end of each experiment, hippocampal neurons plated on coverslips or 35 mm glass-bottom dishes were rinsed briefly in PBS and

fixed with 4% paraformaldehyde (PFA) and 4% sucrose in PBS-MC (PBS with 1 mM $MgCl_2$ and 0.1 $CaCl_2$) for 10 min at room temperature. Neurons were then rinsed three times with PBS-MC and subsequently blocked and permeabilized with blocking buffer containing 2% BSA and 0.2% Triton X-100 in PBS-MC for 20 min. After rinsing neurons three times with PBS-MC, primary antibodies were added in blocking buffer and cultures were incubated overnight at 4°C. The following antibodies and dilutions were used for immunofluorescence stainings: mouse anti-PSD-95 (1:500), rabbit anti-Synapsin I (1:2000), mouse anti-Bassoon (1:2000), rabbit anti-Shank (1:2000), rabbit anti-GluR1 (1:20), chicken anti-Map2 (1:5000), and mouse anti-Myc (1:1000). After three washes with PBS-MC, neurons were incubated in goat anti-rabbit, -mouse, or -chicken secondary antibodies conjugated to Alexa 488, Alexa 568, or Alexa 678 (1:500 each; Invitrogen) at room temperature for 1 h. Neurons were washed three times with PBS-MC and mounted on slides with Aqua Poly/Mount (Polysciences).

Western blot analysis

Cultured neurons were lysed in radioimmunoprecipitation assay (RIPA) lysis buffer (50mM Tris, pH7.4, 150mM NaCl, 1% Triton X-100, 0.1% SDS, 1 mM EDTA) containing protease inhibitors (Roche). Rat or mouse brains

were homogenized in RIPA buffer at 900 rpm in Teflon-glass homogenizers. Neuronal cell lysates or brain homogenates were centrifuged at 14,000 rpm, and supernatants were removed and protein concentration was determined by BSA protein assay kit (Pierce) using bovine serum albumin as a standard. Protein samples were resolved by SDS-PAGE and electrophoretically transferred to nitrocellulose membranes. Membranes were then blocked for 1 h in TBST blocking buffer (TBS, 0.1% Tween 20, and 5% milk) at room temperature and then incubated with primary antibodies in blocking buffer overnight at 4°C. The antibodies used were at the following dilutions: mouse anti-UCH-L1 (1:1000), rabbit anti-ubiquitin (Dako) (1:1000), rabbit anti-CDK5 (1:10,000). Blots were then washed three times in TBST washing buffer (TBS, 0.1% Tween 20) and incubated with goat anti-rabbit, -mouse, or –rat IgG conjugated to horseradish peroxidase (1:5000). Protein bands were visualized by chemiluminescence plus reagent (PerkinElmer) and were digitized and quantified using NIH ImageJ software. For statistical analysis, unpaired Student's *t* test was performed between any two conditions.

Image acquisition and quantification

Confocal images were acquired using a Leica DMI6000 inverted microscope outfitted with a Yokogawa spinning disk confocal head, an Orca ER high-resolution black-and-white cooled CCD camera (6.45 µm/pixel at 1X) (Hamamatsu), Plan Apochromat 40X/1.25 numerical aperture (NA) and 63X/1.4 NA objective, and a Melles Griot argon/krypton 100mW air-cooled laser for 488/568/647 nm excitations. Exposure times were held constant during acquisition of all images for each experiment. Pyramidal-like cells were chosen in a random manner. Confocal *z*-tacks were taken at 0.5-1 µm depth intervals in all experiments. For image analysis, maximum *z*-projections were used. Images were thresholded equally 1.5–2 times above background. Dendrites from individual neurons were then straightened and used for analysis. Fluorescence intensity associated with presynaptic and postsynaptic protein puncta was measured to determine the size and number of puncta (normalized to dendritic length) in control, LDN-treated, and RNAi expressing neurons and C6 cells. To determine the length of a spine, the distance from the tip of the protrusion to the dendritic shaft was measured manually. To measure the width of a spine, the maximal length of the spine head perpendicular to the long axis of the spine neck was measured. The number of spines visible along the dendrite was counted manually per 1 µm dendritic length. Measurements were then

automatically logged from NIH ImageJ into Microsoft Excel. Statistical significance was determined by unpaired two-tailed Student's *t* test. All imaging and analysis of ubiquitin rescue experiments were performed in a blinded manner.

Cell culture and transfection

HEK 293T cell line and C6 rat glial cell lines were maintained in Dulbecco's modified Eagle's medium (DMEM) supplemented with 10% fetal bovine serum, L-glutamine, and penicillin-streptomycin. Transient transfections were performed using Lipofectamine™ 2000 (Invitrogen) according to the manufacturer's protocol. Cells were grown at 37˚C in 5% CO_2.

***In vitro* ubiquitin binding experiment**

UCH-L1 mutants were cloned into BamH I and Xho I sites of pGEX4T-2 vector, which expresses GST protein N-terminal to UCH-L. Bacterially expressed GST and GST-UCH-L1 were purified using GSH beads. In case of the pre-treatment experiment the beads, were incubated with LDN (50 μM) or vehicle (DMSO) in GST binding buffer (25 mM Tris-HCl pH 7.5, 150

mM NaCl, 2 mM EDTA, and 0.5% NP-40) for 30 min in RT provided with gentle rotation. At the end of this incubation period, 10 µg of ubiquitin (Sigma) was added and the mixture was allowed to rotate for another 2 hrs. After which, 2X sample buffer was added and the mixture was boiled for 10min. Samples were resolved on SDS-PAGE and transferred onto nitrocellulose paper. In case of the post-treatment experiment, first 10 µg of ubiquitin was added to the beads and allowed to rotate in RT for a total of 2 hrs. Post treatment with LDN or vehicle, as explained above, was performed 30 mins to 1 hr prior to the end of the 2 hr total incubation period. Samples were resolved the same way as the pre-treatment experiment. The blots for of the experiments were probed for anti-ubiquitin and anti-UCH-L1 antibodies.

In vivo ubiquitin binding experiment

UCH-L1^{WT}-GFP or UCH-L1^{mutant}-GFP were co-transfected with HA tagged ubiquitin into HEK 293T cells. After about 24 hours of expression, cultured cells were treated with 25µM LDN-57444 for 12 hours. Cells were then lysed in a stringent binding buffer (1X Precipitation Buffer, 1%Trx-100, 25mM NEM, 25µM MG132, 0.1% SDS, and proteasome inhibitor). Later they were immunoprecipitated using GFP antibody. IPs were resolved on 4-20%

gradient gel. After transferring the gel onto a nitrocellulose paper, the blot was initially immunolabeled anti-HA antibody. Later it was stripped and immunolabeled with anti-UCH-L1 antibody. Precipication Buffer, PB, contains: 10mM Sodium Phosphate, pH 7.4, 5mM EDTA, 5mM EGTA, and 100 mM NaCla.

RESULTS

Activity dependant up-regulation of UCH-L1 in neurons

An interesting study published in 2006 in *Cell* (36) demonstrated that activation of UCH-L1 is essential for normal synaptic function. In this study UCH-L1was pharmacologically inhibited using a drug called LDN-57444 (LDN) which is a reversible, competitive, active site-directed inhibitor. This drug has high specificity for UCH-L1, IC_{50} value of 0.88 μM, compared to its systemic isoform UCH-L3, IC_{50} value of 25 μM (48). Two hrs perfusion of hippocampal slices with 5 μM LDN resulted in diminished LTP in the CA3-CA1 connections. This finding is suggestive of the fact that UCH-L1 may have a function at synapses. Since synaptic excitability was altered when UCH-L1 was inhibited, we hypothesized that the activity of synapses may be somehow linked to UCH-L1 function. To test this, we monitored UCH-L1 level of activity using a Hemmagglutinin-tagged ubiquitin-vinyl methyl ester-derived active site-directed probe (HAUb-VME) which covalently modifies DUBs including UCHs (64). The C-terminus of the ubiquitin in this probe is linked to a thiol-reactive group (VME) which provides a nucleophilic substitution site for catalytic cysteine residues of active DUBs (figure 1). Moreover the N-terminus side of ubiquitin is linked to a HA tag. If a DUB is in its active form the substitution reaction occurs generating a

covalently linked DUB to the HA-tagged ubiquitin from the probe. Once reaction samples are resolved on SDS-PAGE gel and probed with an anti-HA antibody, only the DUBs that were in the active state will be labeled.

Using this highly sensitive assay which was specifically targeted to detect active UCH-L1, we were able to monitor the UCH-L1 level of activity in lysates generated from rat brain. To test whether UCH-L1 activity might be regulated by synaptic activity, we stimulated neuronal dissociated cell cultures (DIV 21) with NMDA receptor agonist. Synaptic stimulation induced by NMDA/glycine application resulted in significant upregulation of UCH-L1activity (figure 2A; compare the left and right panels). UCH-L1 by itself normally travels at about 25kDa, however the covalent attachment of the HAUb-VME probe to UCH-L1 causes it to travel at about 35kDa. Figure 2B shows a comparison between the active (labeled) and non-active (unlabeled) UCH-L1 in response to NMDA receptor stimulation. As seen, there is a significant shift in the activity of UCH-L1 in which this DUB becomes much more active in case of NMDA induced synaptic activation. Densitometry analysis for this experiment revealed that the level of active UCH-L1 rises from 19% to about 90% when NMDA receptor agonist is applied for 10 min (figure 2B an 2C). To further asses the specificity of our treatment and see if this upregulation of UCH-L1 is due to NMDA receptor activation, we used an NMDA receptor

antagonist. APV, (2R)-amino-5-phosphonovaleric acid, is a selective NMDA receptor antagonist that competitively inhibits the active site of NMDA receptors. Indeed, compared to control the activity of UCH-L1 remained unchanged when NMDA/Gly was applied to APV pretreated neurons (figure 3A). On average, the activity of UCH-L1 increased by about 1.5 folds in response to NMDA receptor stimulation (control, 1.0 ± 0.07; NMDA/Gly, 1.63 ± 0.003; $p = 0.003$, one-way ANOVA) (figure 3B). These data suggest that UCH-L1 is partially active in total lysates from cultured neurons and that NMDA receptor stimulation rapidly increases UCH-L1 activity.

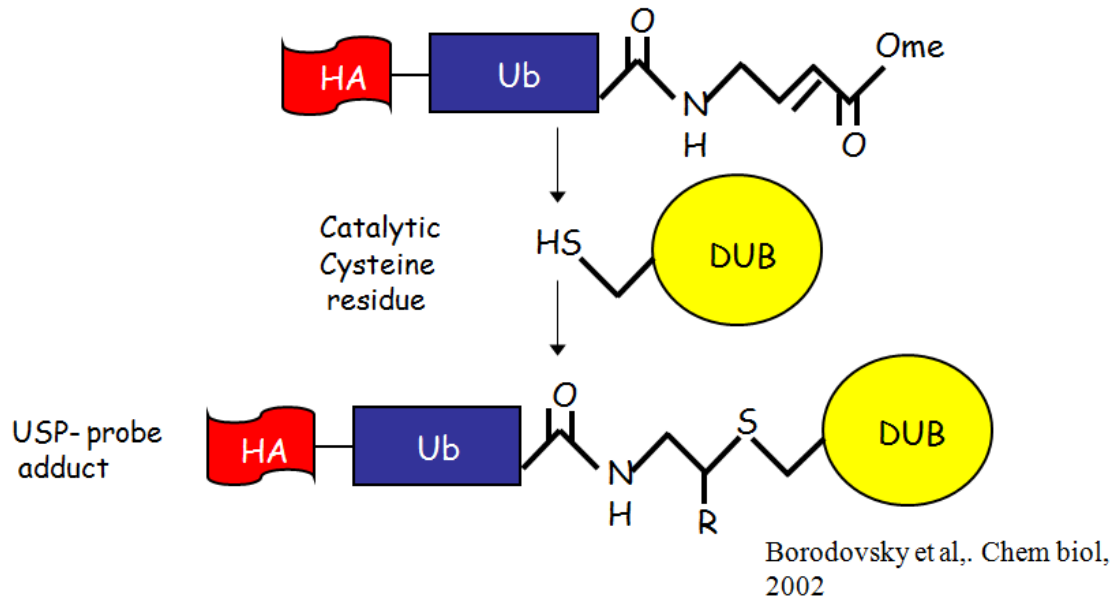

Figure 1: Structure of DUB-specific activity probe (HAUb-VME)

This DUB-specific probe was used to asses the activity level of UCH-L1 within cells. An HA tag, used for probing, is at the N-terminus of a ubiquitin molecule. Moreover, there is a thiol-reactive group at its C-terminus. The C-terminus is able to react with the catalytic cysteine residue of DUBs in their active state and covalently modify them. The HA tag is then used to probe for active DUBs by Western blotting. The HA positive DUBs represent the population of the active DUBs.

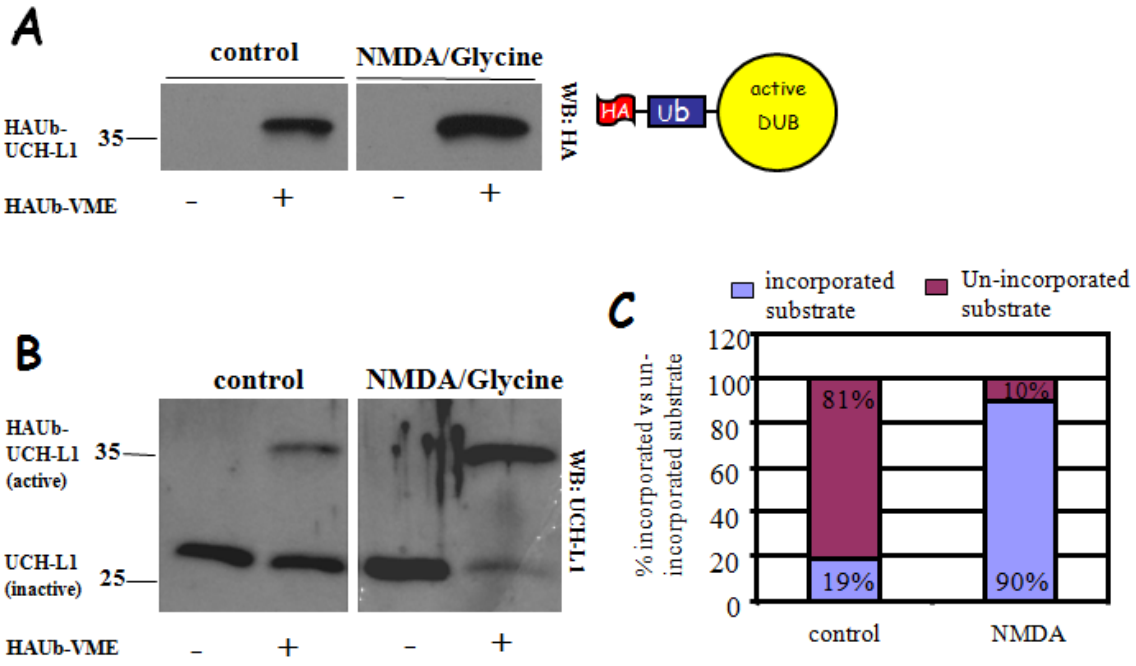

Figure 2: NMDA receptor activation upregulates UCH-L1 activity.

Cultured neurons were treated with 50μM NMDA/10 μM glycine. Lysates from control and treated neurons were labeled with HAUb-VME substrate and subjected to Western blot analysis. ***A,*** A representative immunoblot probed with anti-HA antibody demonstrates the levels of labeled (active) UCH-L1 in control and treated neurons in the presence or absence of the DUB labeling reagent. The blot was subsequently stripped and re-probed with anti-UCH-L1 antibody to demonstrate the levels of labeled and unlabeled UCH-L1 (HAUb-UCH-L1 and UCH-L1, respectively) (***B***). ***C***,Densitometry analysis of DUB labeling assay shown in part A.

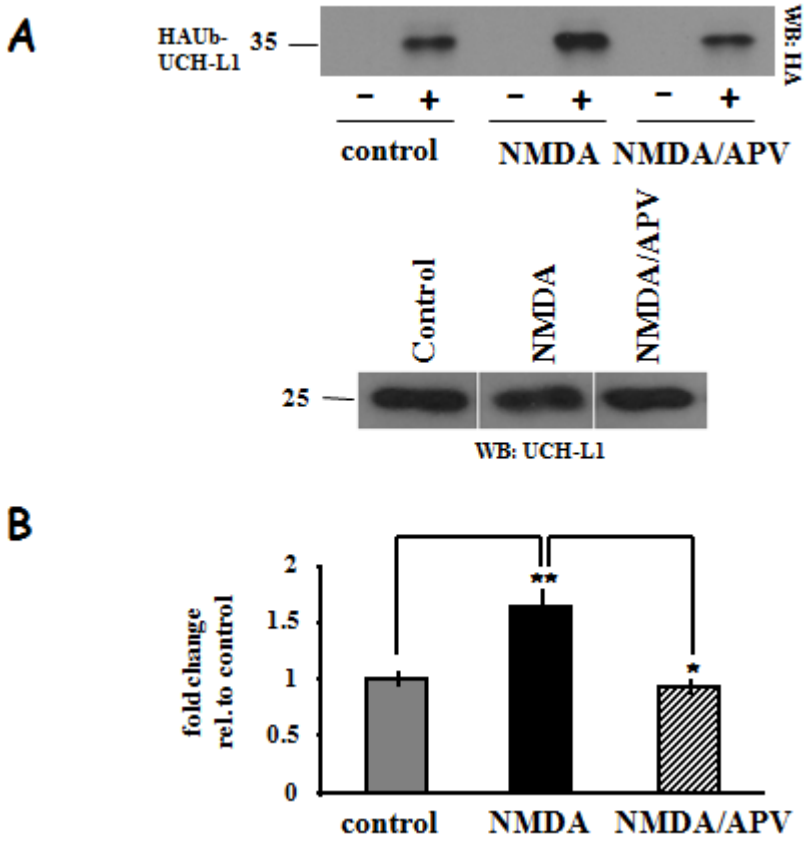

Figure 3: The NMDA mediated activity dependent upregulation of UCH-L1 activity is revered by using APV.

This time in addition cultured neurons were treated with 50μM NMDA/10 μM glycine plus 50μM APV for 10 minutes. ***A***, A representative immunoblot probed with anti-HA antibody demonstrates activity levels of UCH-L1 in response to drug treatment (upper panel). Application of NMDA plus APV, an NMDA blocker, seems to not have any affect on the levels of active UCH-L1. The bottom panel of ***A*** shows equal amount of UCH-L1 between treatments. ***B***, Densitometry analysis of six independent experiments from DUB labeling assay is shown. The bars represent the levels of UCH-L1 activity compared to the control. For statistical analysis, one-way ANOVA with *post hoc* Bonferroni's multiple-comparison test was used. *$p<0.05$; **$p<0.01$.

Activity dependant increase of free monomeric ubiquitin levels in neurons is dependent on UCH-L1 activity

Multiple functions of UCH-L1 have been discovered both *in vivo* and *in vitro*. As described in the introduction section, through its hydrolase ability, UCH-L1 is able to generate free monomeric ubiquitin from precursor ubiquitin polypeptides (54). Provided the large quantity of UCH-L1 in neurons, 1-2% of total protein, we wondered whether altered UCH-L1 activity has any effect on the levels of free monomeric ubiquitin in the cell. To test this we stimulated cultured neurons with 50 μM NMDA/ 10 μM glycine for 10 min and compared the free ubiquitin levels to that of vehicle (DMSO) treated neurons. Neurons were lysed and probed with anti-ubiquitin antibody after resolving and transferring the gel. The result indicates that stimulation with NMDA receptor agonist increases free monomeric ubiquitin levels by approximately two folds compared to control (figure 4). Next, we wanted to see if inhibiting UCH-L1 will have the opposite effect. To asses this, previously described UCH-L1 specific inhibitor LDN was used. After determining the efficacy of the drug, cultured neurons were pre-incubated with 10 μM LDN overnight. The next day, they were either treated with DMSO or stimulated using the same protocol as previous. Neurons treated with LDN showed significant decrease in monoubiquitin levels, average of 40% reduction (control, 1.0 ±

0.11; LDN-treated, 0.59 ± 0.01). Moreover, the levels of free monomeric ubiquitin in neuronal cultures pre-treated with LDN prior to NMDA receptor stimulation were reduced to the levels observed in control untreated neurons (Fig. 2*F*, control, 1.0 ± 0.02; LDN-treated, 0.64 ± 0.05; NMDA/Gly-treated, 2.0 ± 0.13; NMDA/Gly + LDN-treated, 1.04 ± 0.08; $p < 0.001$, one way ANOVA). Altogether, this data suggests that NMDA induced increased neuronal activation leads to an increase in the levels of free ubiquitin in an UCH-L1-dependent manner.

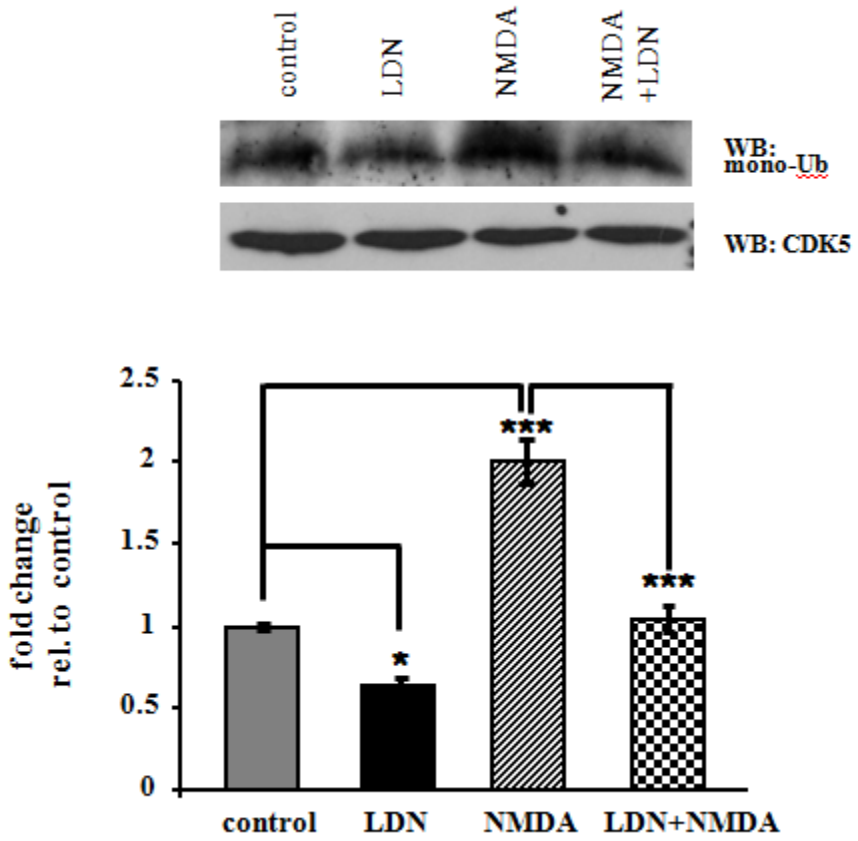

Figure 4: Activity dependent upregulation of free monomeric ubiquitin levels in neurons is associated with UCH-L1 activity.

Cultured neurons were treated with 50µM NMDA/10 µM glycine for 10 minutes or with 10 µM UCH-L1 inhibitor (LDN) for 24 hours with or without an additional 10 min treatment with 50µM NMDA/10 µM glycine. Lysates were resolved on 15% SDS-PAGE and immunoblots were probed with anti-ubiquitin antibody. Representative blots from each experiment are shown. CDK5 probing was performed to show equal loading of the total protein amount on the gel. Relative band intensities of corresponding monomeric ubiquitin were quantified and are depicted in the bottom panel of the figure. The bars represent the ubiquitin levels with respect to the control. For statistical analysis, one-way ANOVA with *post hoc* Bonferroni's multiple-comparison test was used. *p<0.05; **p<0.01; ***p<0.001.

Pharmacological inhibition of UCH-L1 activity leads to changes in synaptic structure

As viewed by electron microscopy, post synaptic density (PSD) was first identified as an electron-dense region at the membrane of a postsynaptic neuron. The PSD is highly dynamic, changing its size and composition throughout development and in response to synaptic activity. It has been widely accepted that modifications to the PSD composition over the time scale of seconds to hours is thought to underlie both long-term potentiating (LTP) and long-term depression (LTD) (30, 65). Moreover, studies using previously explained *gad* mice and LDN treated hippocampal slices have demonstrated that UCH-L1 is required for LTP and maintenance of memory (36, 66). Taken together, these findings suggest that UCH-L1 may play a role in the modification of the PSD composition. To examine this possibility we compared the immunocytochemical distribution of several synaptic proteins in control and LDN treated cultured neurons. Although *gad* mice show no gross structural abnormalities, we found that exposure of mature hippocampal neurons to LDN leads to dramatic alterations in synaptic structure (figure 5). It has been known that post-synaptic proteins PSD-95 and shank are targeted for degradation by the UPS in an activity dependent manner (33, 67-69). Therefore we labeled for these protein clusters to observe their

distribution with and without the presence of UCH-L1 inhibitor, LDN. We observed a significant increase in the size of these protein clusters. Also detected was an increase in the size of pre-synaptic protein puncta as measured by immunolabeling for pre-synaptic nerve terminals with Synapsin I and Bassoon (figure 5). As for the post-synaptic proteins, on average, the size of PSD-95, shank, and GluR1 puncta increased by 77%, 70% and 39%, respectively (Fig. 6A, PSD-95 puncta, control, 1.0 ± 0.03; LDN-treated, 1.77 ± 0.04; Shank puncta, control, 1.0 ± 0.04; LDN-treated, 1.69 ± 0.04; surface GluR1 puncta, control, 1.0 ± 0.07; LDN-treated, 1.39 ± 0.08). For the pre-synaptic proteins, we found that on average, there was a 34% and 25% increase in the size of Synapsin I and Bassoon puncta, respectively (Fig. 6A, Synapsin I puncta, control, 1.0 ± 0.05; LDN-treated, 1.34 ± 0.07; Bassoon puncta, control, 1.0 ± 0.03, LDN-treated, 1.25 ± 0.02). Interestingly, no change was observed in the dendritic protein marker MAP2 staining when comparing control to LDN treated neurons. This may suggest that while UCH-L1 affects synaptic protein structures, it has no effect on the overall integrity of the dendrites.

In addition to analyzing the size of the pre- and post-synaptic protein clusters, we also examined to see if there is a change in the density of the synaptic protein puncta. The analysis revealed that the density of PSD-95 puncta was decreased by 30% (figure 6B control, 1.0 ±

0.04; LDN-treated, 0.8 ± 0.3). However, no significant changes were observed comparing the density of Shank, surface GluR1, Synapsin I and Bassoon puncta in the LDN treated neurons to that of control (figure 6B).

Additionally, since spine size is directly proportional to the area of the post-synaptic density (PSD) (70-71), we wanted to see if the observed alterations in the synaptic protein clusters could possibly be accompanied by any changes in spine size and density. To detect alterations in the size of the spines, we analyzed spines from GFP-expressing neurons which were treated with either LDN or vehicle (DMSO). A dramatic alteration in the size of spines in the LDN-treated neurons was observed. Neuronal spines enlargement of about 80% in spine head width and 37% increase in spine length was revealed (fig. 6C, spine head width, control, 1.0 ± 0.09; LDN-treated, 1.8 ± 0.22; fig. 6D, spine length, control, 1.0 ± 0.03; LDN-treated, 1.37 ± 0.08). Furthermore, we found that blocking UCH-L1 activity dramatically reduced the number of spines (figure 6E). The LDN-treated neurons had approximately 50% reduction in the number of spines as compared to the control untreated neurons (spines/micron: control, 0.72 ± 0.05; LDN-treated, 0.35 ± 0.05). These data are suggestive of the fact that alterations in synaptic structure, induced by inhibition of UCH-L1 activity, are also accompanied by changes in spine morphology.

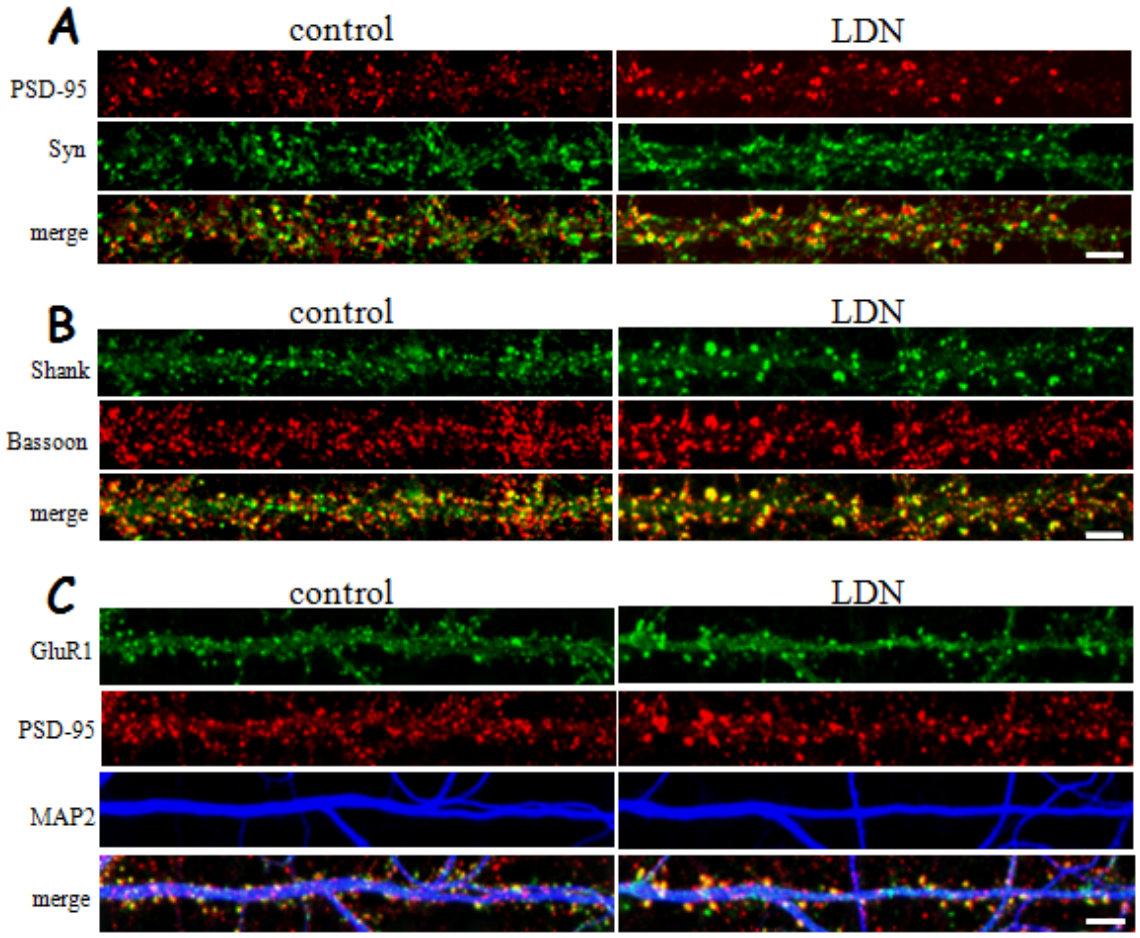

Figure 5: Pharmacological inhibition of UCH-L1 activity leads to alteration of synaptic structure.

Cultured neurons were treated with LDN for 24 hours. At the end of LDN treatment, neurons were fixed, permeabilized, and immunolabeled with anti-PSD-95 and anti Synapsin I antibodies (**A**), anti-Shank and anti-Bassoon antibodies (**B**), or live-labeled with anti-GluR1 for surface GluR1 staining, and then fixed and stained with anti-PSD-95 and anti-MAP2 antibodies (**C**). Representative maximum z-projected confocal images and straightened dendrites from control and LDN-treated neurons are depicted. Scale bar, 5μm.

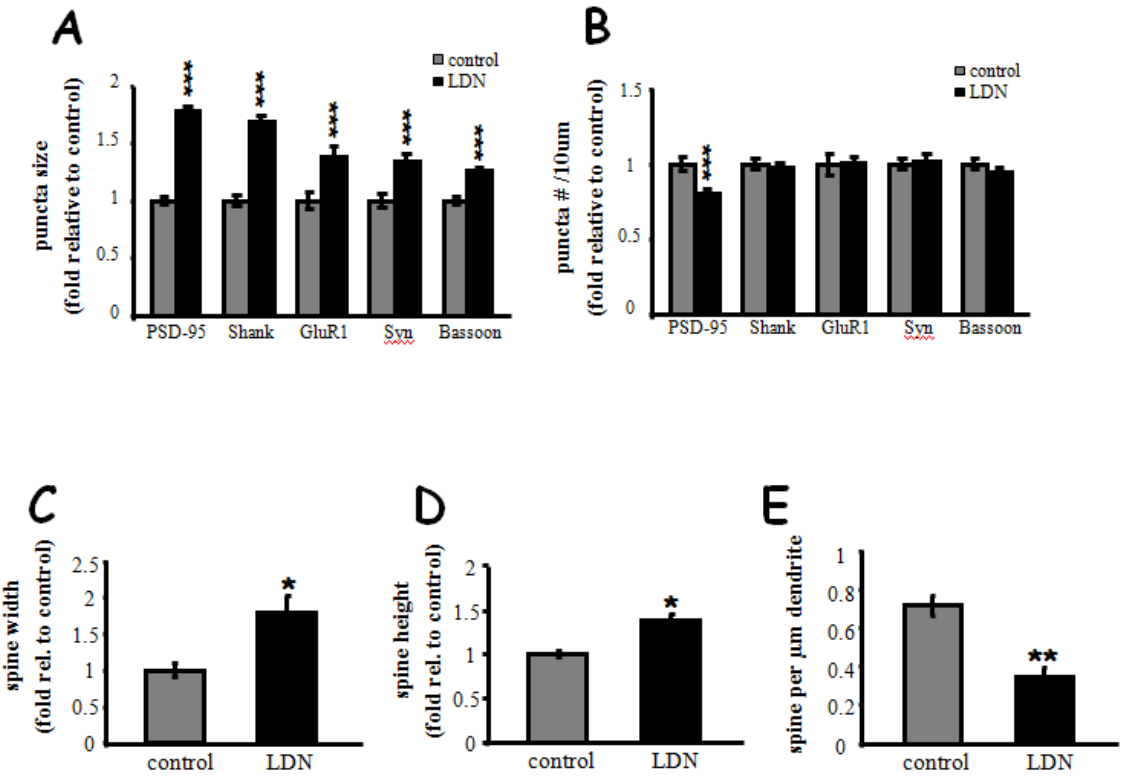

Figure 6: Quantification of the alterations in synaptic protein puncta size and spine size upon UCH-L1 inhibition using LDN.

A, B, Presynaptic and postsynaptic protein puncta size and number were analyzed in control and LDN-treated neurons. The mean puncta size and number in LDN-treated neurons were normalized to those of control neurons from three to four independent experiments. ***C, D,*** Measurments for spine head widths and spine lengths were normalized to those of control values. ***E***, Quantification of spine density is represented as the number of spines per 1µm dendrite length. Mean values ± SEM are shown. For statistical analysis, unpaired Student's *t* test was performed between any two conditions. ***p<0.001; **p<0.01; *p<0.05.

Ubiquitin over-expression in UCH-L1 inhibited culture hippocampal neurons restores the alteration seen synaptic structure

As the most abundantly expressed soluble protein in the brain, UCH-L1 plays an important role in global ubiquitin-dependant UPS function in neurons (61). As mentioned earlier, one of the main functions of UCH-L1 is generation of monomeric ubiquitin from precursor ubiquitin molecules which is subsequently used for various cellular processes. Our data demonstrated that application of UCH-L1 specific inhibitor, LDN, lead to a reduction in the levels of free monomeric ubiquitin in neurons (figure 4). Furthermore, we observed significant changes of spine and synaptic structure when the same drug was applied to cultured neurons (figure 5). Taken together, these data is suggestive of the fact that perhaps the synaptic structural changes seen in UCH-L1 inhibited neurons are, at least in part, attributable to the reduction in the levels of free monomeric ubiquitin. To determine this possibility we performed rescue experiments in LDN-treated neurons (figure 7). Indeed, expression of ubiquitin for twelve hours completely rescued the effects of UCH-L1 inhibition on PSD-95 size and distribution. As was observed previously, PSD-95 puncta size was increased in LDN-treated neurons (figure 7B); however, this increase was completely blocked in myc-ubiquitin expressing neurons (figure 7D). Analysis of the PSD-95 puncta size on straightened dendrite from these

neurons confirmed our observations (figure 8A, GFP-DMSO, 1.0 ± 0.05; ubiquitin-DMSO, 0.93 ± 0.04; GFP+LDN, 1.6 ± 0.04; ubiquitin+LDN, 1.0 ± 0.03). Moreover, the analysis revealed that while there was a slight decrease in the density of PSD-95 puncta in LDN-treated neurons, there was no significant difference in the density of PSD-95 puncta between control (GFP and DMSO-treated neurons) and myc-ubiquitin expressing neurons (Fig. 8B, GFP-DMSO, 1.0 ± 0.04; ubiquitin-DMSO, 0.97 ± 0.05; GFP+LDN, 0.89 ± 0.03; ubiquitin+LDN, 1.1 ± 0.03).

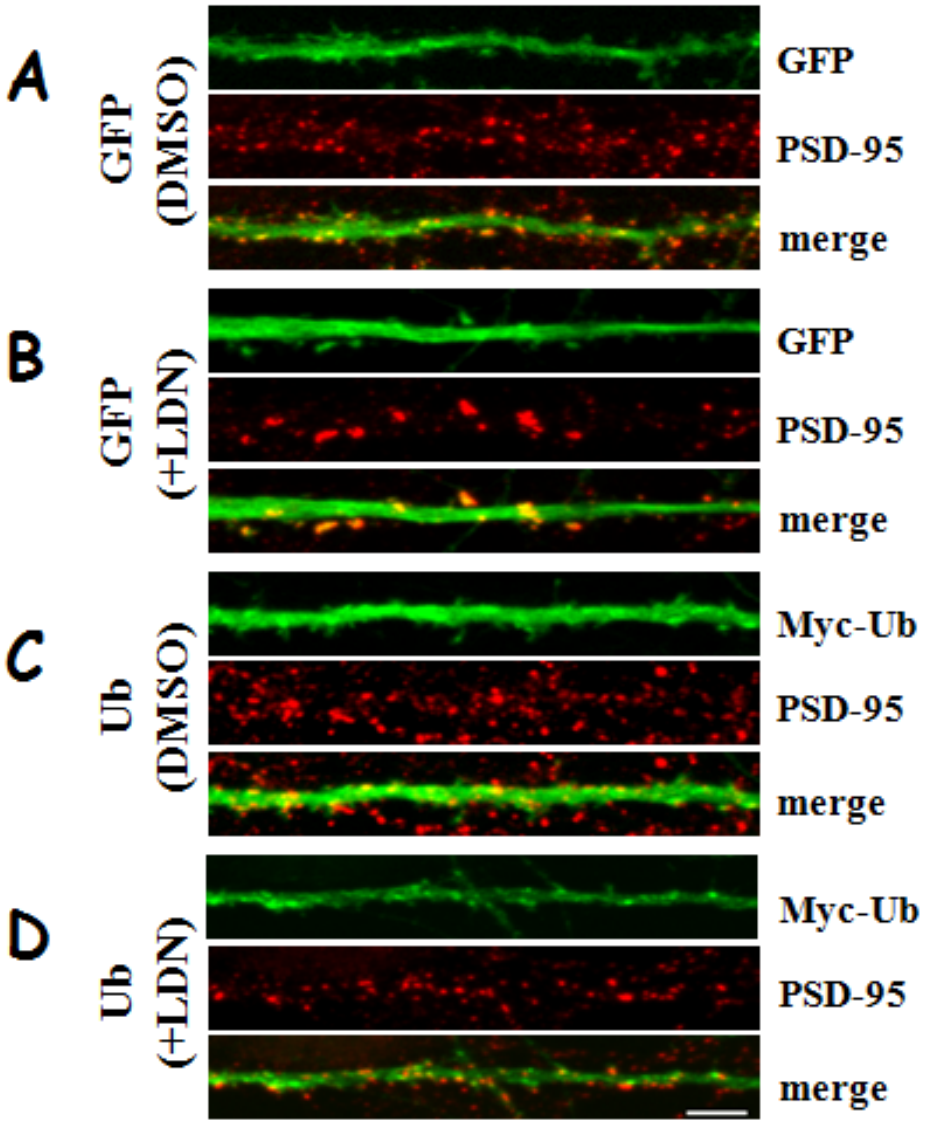

Figure 7: Overexpression of ubiquitin restores the synaptic structure seen in LDN-treated neurons.

Cultured neurons were treated with vehicle (DMSO) or LDN for 24 h. EGFP or Myc-ubiquitin Sindbis virions were added directly to culture media after 12 h of treatment, and protein expression was allowed to continue for 12 h. At the end of the treatments, neurons were fixed, permeabilized, and immunolabeled with anti-PSD-95 or co labeled with anti-PSD-95 and –Myc antibodies. ***A-D***, Representative maximum z-projected confocal images of straightened dendrites from GFP (DMSO), GFP (+LDN), myc-ubiquitin (DMSO), and myc-ubiquitin (+LDN) respectively.

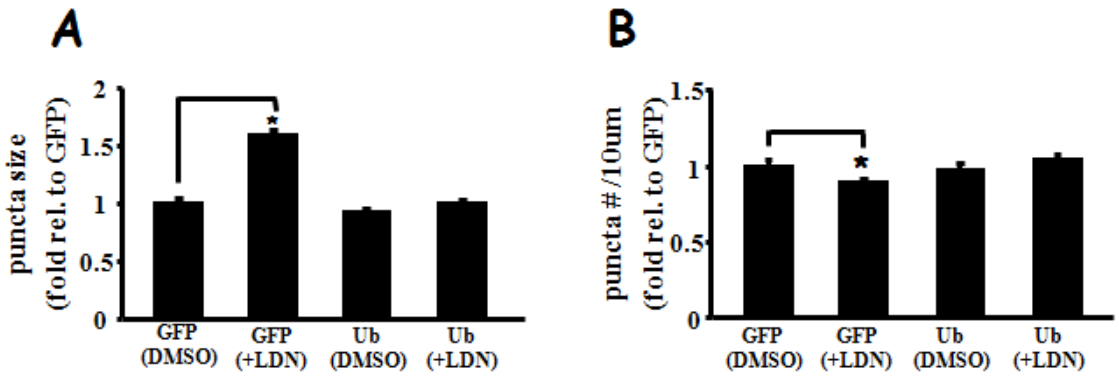

Figure 8: Quantification of the alterations in synaptic protein puncta size and density upon UCH-L1 inhibition using LDN and overexpression of myc-ubiquitin.

PSD-95 protein puncta size (***A***) and number (***B***) were analyzed in neurons that expressed EGFP or myc-ubiquitin The mean puncta size and the number from three different independent experiments were normalized to the GFP (DMSO) control. The number of puncta was calculated per 10µm dendrite length. Measurements for PSD-95 staining were made of >60 dendrite per condition . Scale bar, 5µm. Mean value ± SEM are shown. *p<0.05, **<0.001, unpaired Student's *t* test.

Effect of altered UCH-L1 activity on levels of free monomeric ubiquitin

Our data have thus far demonstrated that inhibiting UCH-L1 leads to reduction in the levels of monomeric ubiquitin in cells. Furthermore, this reduction in neurons may be the underlying reason behind the observed changes in synaptic structure. To better understand the mechanism behind LDN effect on UCH-L1 function, we wanted to see if overexpression of UCH-L1 mutants can have any similar effect on the levels of monomeric ubiquitin in cells. To perform this test, we generated a GFP tagged version of UCH-L1^{WT}-GFP, as well as two mutants: UCH-L1^{C90S}-GFP and UCH-L1^{D30A}-GFP constructs. The UCH-L1^{C90S} mutation, in which the 90th amino acid has been substituted from a cysteine to a serine, lacks ubiquitin carboxy-terminal hydrolase activity but retains the ability to bind ubiquitin (55). The UCH-L1^{D30A} mutation, in which the 30th amino acid has been substituted from an aspartic acid to an alanine, is deficient in hydrolase activity and in addition is unable to bind monoubiquitin (49). The inability to bind ubiquitin is believed to be due to a charge reversal on the surface of the protein that is presumed to interact with cationic residues of Ubiquitin (72). These constructs were used to transfect HEK293T cells for forty-eight hours. Next, cells were lysed and immunoprecipitated using anti-GFP antibodies. All of our constructs were expressed equally, (Figure 9A, upper panel). Furthermore, using the previously explained DUB

activity labeling probe HAUb-VME, it was revealed that only UCH-L1^{WT}-GFP has hydrolase activity (Figure 9A, lower panel). The absence of any band in the anti-HA immunolabeling of the HAUb-VME treated blot in the case of UCH-L1^{C90S}-GFP and UCH-^{D30A}-GFP indicates that these mutants did not have any hydrolytic activity.

Since it is known that inhibition of proteasome activity can directly affect the levels of ubiquitin-conjugated proteins, we next tested to see if overexpression of UCH-L1 mutants can have any effect on the level of polyubiquitin conjugates. HEK293T cells were transfected much the same way as before for 48 hours and the blot was immune-labeled for ubiquitin conjugates. Comparing the different conditions, the levels of polyubiquitin conjugates did not change significantly (figure 9B, upper panel). This suggests that assessed by using the mentioned mutants, catalytic activity of the proteasome are not affected by altered UCH-L1 function. Interestingly, however, the levels of mono-ubiquitin were altered in the overexpression experiments. There was approximately a 4-5-fold increase in the levels of free monomeric ubiquitin in cells overexpressing wild type and the C90S mutant of UCH-L1 (Figures 9B, middle panel, and 9C, GFP, 1.0 ± 0.16; wild type UCH-L1, 4.3 ± 0.23; C90S-UCH-L1, 4.7 ± 0.67; D30A-UCH-L1, 0.97 ± 0.07). Nonetheless, monomeric ubiquitin levels stayed the same as control in case of UCH-L1^{D30A} mutant. This data is interesting because

while both D30A and C90S lack hydrolytic ability, C90S mutant still maintains its ubiquitin binding ability which is thought to be important in stabilizing ubiquitin levels (49, 73). Taken together, these data suggest that while altered UCH-L1 has no affect on the proteasome catalytic activity, it does however have an effect on the levels of monomeric ubiquitin in cells.

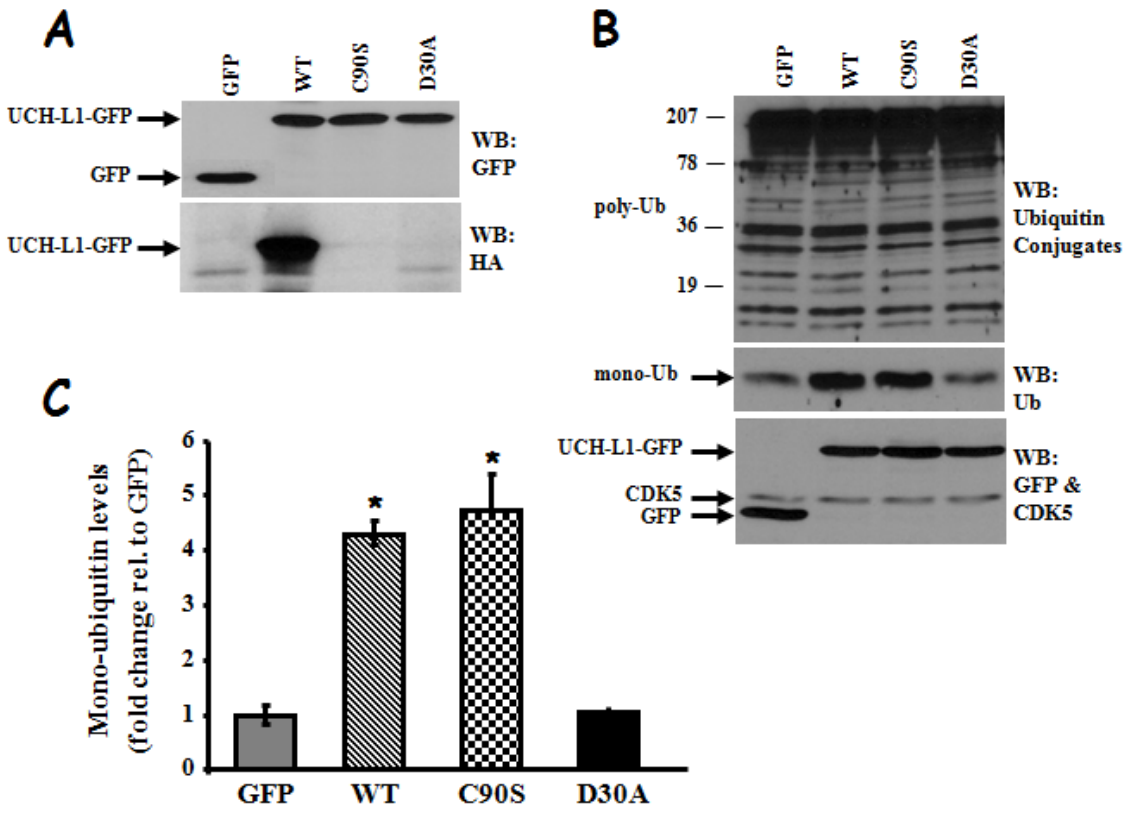

Figure 9: Effects of altered UCH-L1 activity on mono-ubiquitin.

HEK 293T cells were transfected with wild-type, C90S and D30A UCH-L1-GFP constructs for 48 hours. A, Expression levels of GFP, wild type and mutant UCH-L1-GFP were assessed by Western blot analysis. Immunoblots were probed with anti-GFP antibody (top panel). Activity levels of wild-type and mutant UCH-L1-GFP were assessed by DUB labeling assay (HAUb-VME) of lysates from HEK 239T-transffected cells. Bottom panel shows a representative Western blot of labeled lysates. B, Expression levels of free monomeric ubiquitin and polyubiquitin conjugates in transfected HEK 239T cells are shown. Western blot probed with anti-UCH-L1 and anti CDK5 (loading control) antibodies demonstrating equal expression of wild-type and mutant UCH-L1-GFP and equal protein loading, respectively. C, Relative intensities of free monomeric ubiquitin levels in GFP , wild-type, and mutant UCH-L1-GFP transfected cells obtained by densitometry analysis of ubiquitin blots from three independent experiments. Mean values ± SEM are shown. *$p<0.01$, unpaired Student's t test between control (GFP) and any test group.

LDN-57444 affects the binding ability of UCH-L1 *in vitro*

The observed changes in the levels of monomeric ubiquitin upon UCH-L1 and UCH-L1 variants ectopic over expressions are consistent with previous studies (73). It is important to note again that UCH-L1^{D30A}, which lacks binding ability for ubiquitin, leads to reduced ubiquitin levels in HEK cells compared to UCH-L1^{WT} over expression. Furthermore, studies using lysosomal inhibitors have suggested that ubiquitin degradation occurs in lysosomes and that through its ubiquitin binding ability, UCH-L1 is able to increase the half life of Ub by altering its metabolism (49). Taken together, it seems that ubiquitin binding ability of UCH-L1 plays an important role on the maintenance of free ubiquitin in cells. Seeing how we reported reduction in ubiquitin levels in LDN treated neurons, we wanted to test whether LDN has any effect on the ubiquitin binding ability of UCH-L1. To test this hypothesis a few constructs were generated.

Using PCR techniques, UCH-L1^{WT} and UCH-L1^{mutants} cDNA were amplified and through traditional cloning they were introduced into GST containing pGEX4T-2 vector at BamH I and Xho I sites (figure 10A). The DNA was then expressed in DH5a bacteria cells in large quantity and purified using GSH (reduce glutathione) beads. To assure that the GST-UCH-L1 fusion protein is expressed in full, small samples of the purified

protein were resolved on SDS-PAGE gel and stained with Coomassie Brilliant Dye (figure 10B). As expected, GST-UCH-L1 travels at about 50kDa.

Using the generated GST-UCH-L1^{WT} protein, *in vitro* ubiquitin binding assays were designed to assess any possible affect that LDN may have on the ubiquitin binding ability of UCH-L1. In a pre-treatment experiment, GST beads or GST-UCH-L1 beads were treated with 50μM LDN or DMSO for 30 minutes prior to addition of 10μg ubiquitin, which were then allowed to rotate for 2 hours. After boiling the beads for 10 minutes to assure the fusion protein is disattached from the GSH beads, samples were resolved and the transferred blot was probed with anti-ubiquitin antibody, Dako (figure 11A). If UCH-L1 is able to bind to ubiquitin, during the washing of the beads or boiling, the attached ubiquitin will be released and will be visible as free ubiquitin on SDS-PAGE. Compared to DMSO treated beads, the LDN treated ones showed a dramatic reduction in the amount of mono-Ub. This indicates that LDN treated UCH-L1 has reduced ability to bind ubiquitin. Figure 11B is a Coomassie staining of the samples which shows that about the same amount of GST and GST-UCH-L1 protein were used in the binding reaction.

Although *in vitro* experiments, we wanted to create a scenario that resembles what happens inside a cell. Therefore, we performed a post-treatment experiment. Normally in a cell ubiquitin is already present when

LDN is added to the culture. Thus, we made a minor change in our experiment where ubiquitin was first added to the beads with a subsequent addition of LDN. Using three different time points we asked the same question about the effect of LDN on UCH-L1 binding ability toward ubiquitin. We had already shown that GST does not bind ubiquitin, therefore in this experiment only GST-UCH-L1 was used for the binding reactions (figure 11C). Data from the post-treatment experiment demonstrate that the addition of LDN to UCH-L1, even after it has already been incubated with ubiquitin, leads to reduction in the protein's ability to bind ubiquitin. Moreover, longer exposures of UCH-L1 to LDN lead to a greater reduction in the binding ability of the protein. This is potentially a very interesting finding because it demonstrates that even in the case where UCH-L1 has already been incubated with ubiquitin, and therefore presumably has bound to ubiquitin, LDN can potentially disrupt this interaction, leading to the observed reduction in the amount of ubiquitin pull down.

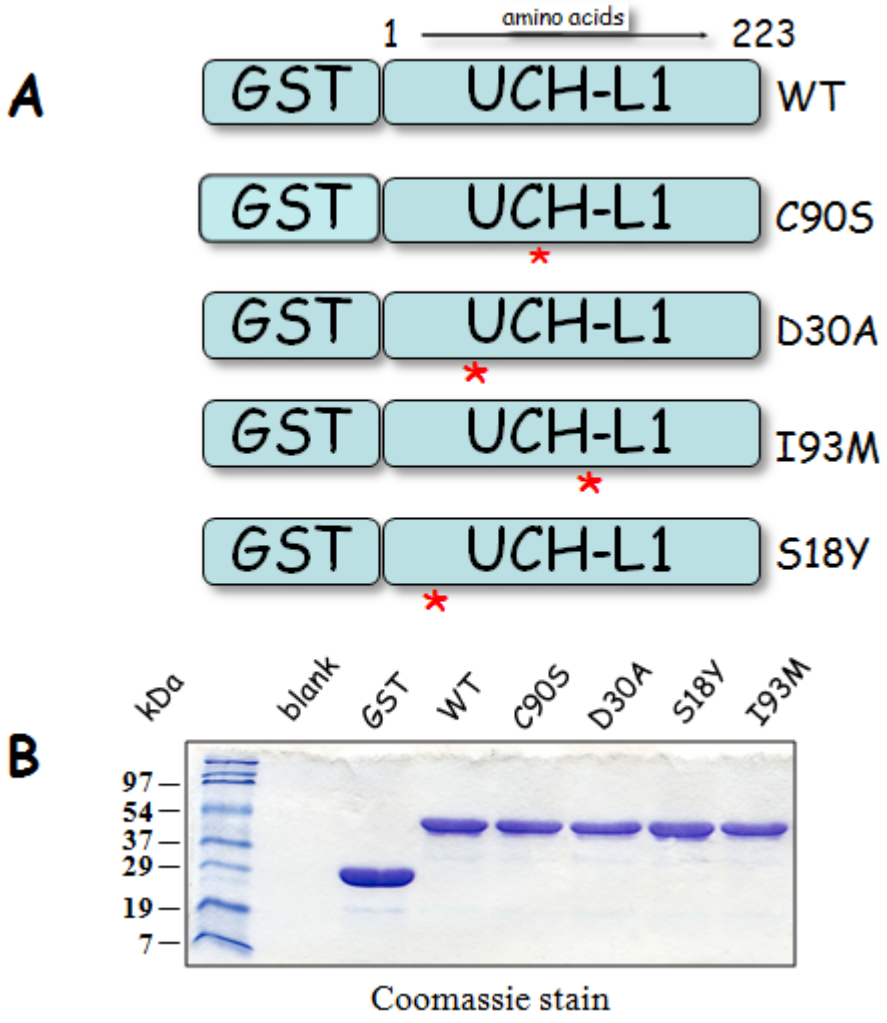

Figure 10: UCH-L1 mutants cloned into pGEX4T-2 vector.

Single point mutations in the UCH-L1 DNA were introduced by PCR-based site-directed mutagenesis of template plasmid cDNA using primers designed to introduce specific mutations. These mutations were then cloned into BamH I and Xho I sites of pGEX4T-2 vector, which expresses GST protein N-terminal to UCH-L1. ***A***, schematic of the constructs. *: represent the sites of mutations. Bacterially expressed GST and GST-UCH-L1 are purified with GSH-beads and were resolved on SDS-PAGE gel to verify full expression (***B).*** Coomassie stain was used to visualize the proteins.

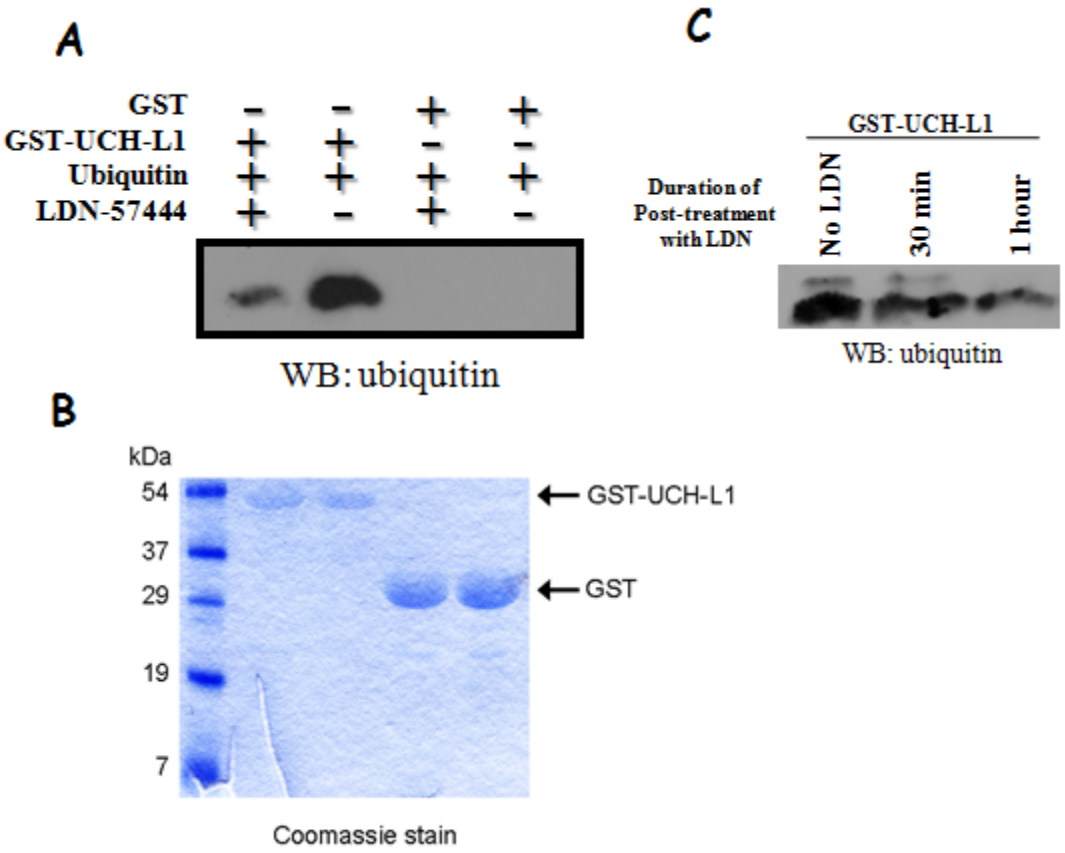

Figure 11: LDN-57444 affects ubiquitin binding activity of UCH-L1, *in vitro*.

Bacterially expressed GST and GST-UCH-L1 (on GSH-beads) were incubated with LDN (50 µM) or vehicle (DMSO) in GST binding buffer (25 mM Tris-HCl pH 7.5, 150 mM NaCl, 2 mM EDTA, and 0.5% NP-40). All reactions were done at RT with gentle rotation. After each reaction the beads were washed 4X with GST binding buffer, boiled in 2X sample buffer, and resolved on 4-15% SDS-PAGE. Nitrocellulose membranes were probed with anti-ubiquitin antibody. ***A***, Beads were pre-treated for 30 minutes prior to incubating with 10 µg of ubiquitin (Sigma) for 2 hrs. GST-UCH-L1 specifically interacts with ubiquitin when compared to GST alone. However, pre-treatment with LDN greatly diminishes the ability of GST-UCH-L1 to bind ubiquitin. ***B***, Coomassie stain showing the amounts of GST-UCH-L1 and GST used in the binding reaction. This blot is representative of 2 independent experiments. ***C***, Beads were incubated with 10 µg of ubiquitin for a total of 2 hrs. During which they were either treated with LDN in the last hour, 30 min, or not at all.

In vitro incubation of purified UCH-L1 with ubiquitin leads to potential UCH-L1 auto-ubiquitination

Aside from the previously described D30A and C90S variants of UCH-L1, there are two more mutations which have been directly associated with PD in patients. A polymorphism in UCH-L1, seen in relatively high frequency among Japanese and Asians, resulting in a substitution of serine 18 to a tyrosine, S18Y, has been reported to be protective against PD (74). The hydrolysis activity of this mutant has been shown to be higher than WT while the ligase activity has been reported to be much less than the wild type. Furthermore, another point mutation, isoleusine 93 to methionine has been associated with a gain of toxic function of UCH-L1 and PD. This mutation has greatly reduced hydrolase activity as well as a reduced ligase activity. These mutations are interesting because they occur naturally in humans and studying their function will be very informative toward better understanding neurodegenerative diseases, specifically PD.

While performing *in vitro* ubiquitin binding experiments using all the generated GST-UCH-L1^{mutant} forms to uncover LDN effects on the protein, surprisingly, we discovered interesting high molecular banding patterns above 50kDa, the normal size of GST-UCH-L1 (figure 12). With the exception of the presence of all the UCH-L1 mutant forms, the setup of this

experiment was identical to the LDN pre-treatment experiment. Long exposures of the blot revealed the high molecular banding pattern to be present in C90S, I93M, WT, and very dimly in the LDN treated S18Y. Although these results warrant performing more experiments of this type, they are potentially very important for a few reasons, some of which are as follows.

The only two proteins in the reaction mixture in these experiments were ubiquitin and UCH-L1, which suggests that the higher molecular bands are correspondent to either multimerization of UCH-L1 or ubiquitination of the protein. While we do not have any data for co-labeling of these bands with ubiquitin antibody, it should be noted that multimerization of UCH-L1 would probably result in more distinct bands rather than the observed smearing. Moreover, the high molecular bands are absent in the GST-UCH-L1^{WT} lane when ubiquitin was not added.

Previous studies have shown that UCH-L1 can be mono-ubiquitinated in cells and that this ubiquitination is reversed by the activity of UCH-L1 itself (75). In line with that finding, we found that the banding patterns are more robust in the mutants that lack hydrolase ability. C90S which has no hydrolase ability has the highest amount of banding, which may be due to the fact that it cannot hydrolyze the ubiquitin from itself. Moreover, the S18Y mutation, which has increased hydrolase ability

compared to the WT, has less banding compared to WT. D30A is an interesting case because even though it lacks hydrolase ability, like C90S, it does not show any high molecular banding pattern. This is probably related to the fact that this mutation eliminates ubiquitin binding which may be required for UCH-L1 ubiquitination.

Lastly, we observed that comparing LDN treated to DMSO treated samples for each mutation, the LDN treated samples showed a greater amount of high molecular banding. This is most likely due to the induced lack of hydrolase ability of UCH-L1 upon LDN application. This phenomenon is most visible when looking at the I93M DMSO and I93M LDN treated lanes. The aforementioned increase banding pattern with the addition of LDN was not noticeable in the case of the C90S mutation. This may be due to the fact that C90S already exhibits no hydrolase ability and therefore the effect of LDN is occluded.

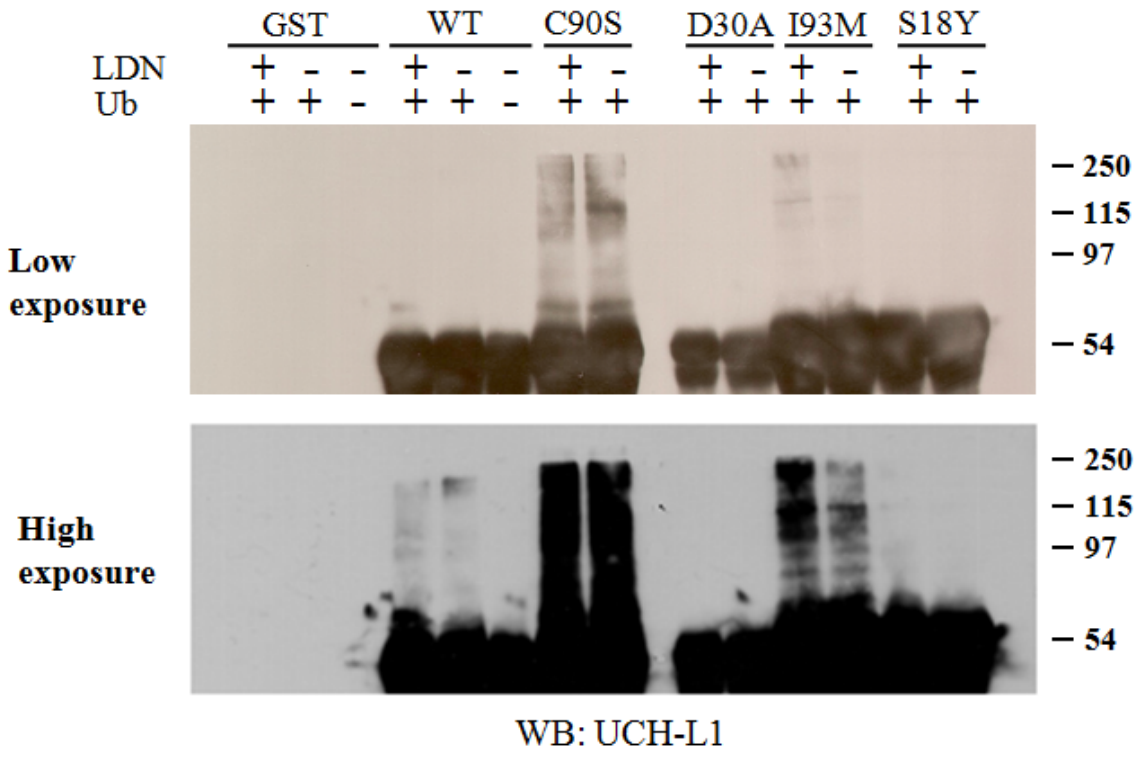

Figure 12: UCH-L1 is ubiquitinated *in vitro*

Bacterially expressed GST and GST-UCH-L1 (on GSH-beads) were incubated with LDN (50 µM) or vehicle (DMSO) in GST binding buffer (25 mM Tris-HCl pH 7.5, 150 mM NaCl, 2 mM EDTA, and 0.5% NP-40) for 30 minutes. Ubiquitin (10 µg, Sigma) was then added and the binding reaction was performed at RT for 2 hours with gentle rotation. The beads were then washed, boiled and resolved on 4-15% SDS-PAGE. The transfer blot was subsequently probed with anti-UCH-L1 antibody. GST-UCH-L1, about 50kDa, can be easily detected in the lighter exposure, top panel. However, with higher exposure, in many of the lanes a smear of proteins positive for UCH-L1 can be detected above 50kDa. Interestingly this pattern is more robust in the C90S and I93M mutants.

LDN-57444 affects the binding ability of UCH-L1 *in vivo*

After learning that LDN diminishes UCH-L1 ability to bind ubiquitin in *in vitro* studies, we wanted to see if this also holds true in cells. To examine this we used UCH-L1^{WT}-GFP and UCH-L1^{mutants}-GFP constructs which were generated by cloning UCH-L1 cDNA into pEGFP vector. The constructs along with HA tagged ubiquitin were co-transfected into HEK 293T cells for 24 hours. Next, they were treated with DMSO or LDN and incubated for an additional 12 hours before lysing the cells in a stringent lyses buffer containing 1% Trx-100 and 0.1% SDS. After probing the blot with anti-HA antibody we observed that given the conditions of our experiment and the stringent binding buffer used, C90S was the only mutant form which was able to bind ubiquitin (figure 13). This indicates that ubiquitin binding interaction is the strongest between UCH-L1^{C90S} and ubiquitin compared to other mutant forms and even WT. Furthermore, we did see that LDN has an effect on the amount of ubiquitin binding. UCH-L1^{C90S}-GFP transfected HEK cells treated with LDN bound less HA-tagged ubiquitin compared to DMSO treated HEK cells. This is an interesting finding because it demonstrates that the reduction in the amount of free ubiquitin seen in LDN treated neurons is not only due to the reduced hydrolytic activity of UCH-L1, which leads to less production of ubiquitin from ubiquitin precursor molecules, but it is also due to a reduction in the binding ability

of UCH-L1 for ubiquitin. The reduced binding ability then can presumably result in increased lysosomal degradation of ubiquitin.

In addition, we also noticed that UCH-L1 is mono-ubiquitinated in the cells. This phenomenon has been previously reported and it has been proposed to play a role in regulating UCH-L1 function (75). Consistent with this study, we also observed that the UCH-L1^{C90S} mutant form is heavily mono-ubiquitinated compared to other mutants. This is thought to be due to the idea that UCH-L1 auto-deubiquitinates itself and that this ability is absent in the case of the catalytically inactive C90S mutation. Our study however is interesting in that we also examined whether LDN can have any effect on the level of UCH-L1 mono-ubiquitination. Probing the blot with anti-HA antibody, which can mark HA-ubiquitinated UCH-L1 protein, revealed that no significant difference exists in the level of mono-ubiquitinated form of UCH-L1 in the LDN treated HEK cells compared to that of the control.

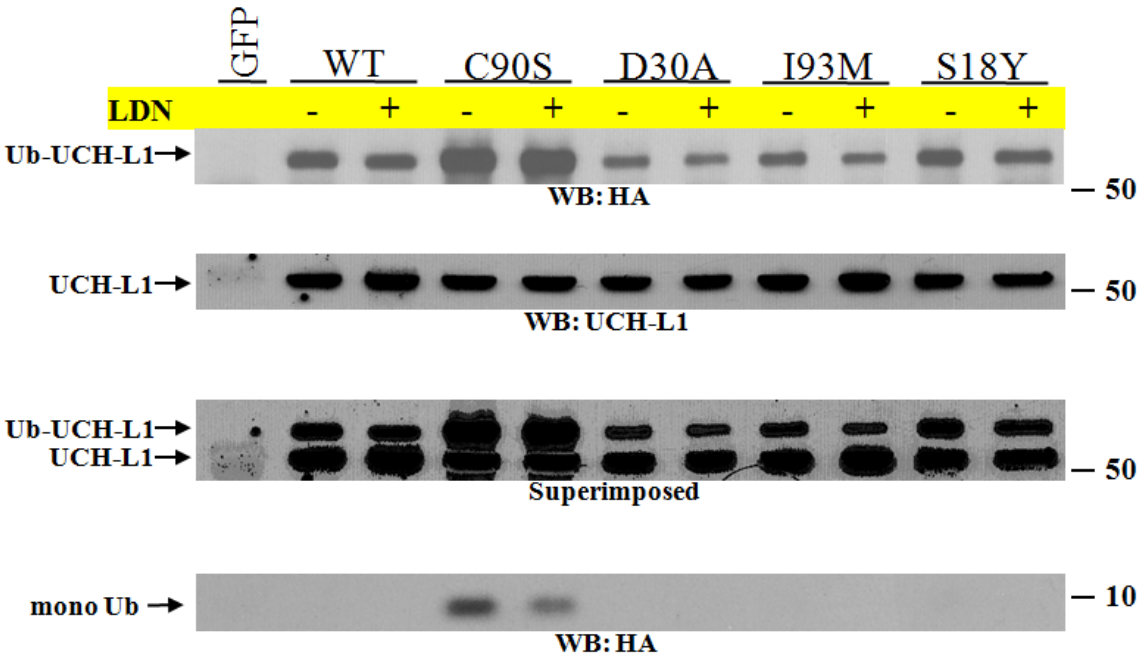

Figure 13: C90S mutant has higher levels of the mono-ubiquitinated form of UCH-L1. In addition, LDN-57444 affects ubiquitin binding activity of UCH-L1, *in vivo*.

HEK 239T cells were co-transfected with UCH-L1-GFP and HA-Ub. After about 24 hours, the cells were treated with 25μM LDN for 12 hours. Then the cells were lysed in a stringent binding condition (1X Precipitation Buffer, 1%Trx-100, 25mM NEM, 25μM MG132, 0.1% SDS, and proteasome inhibitor). After resolving on SDS-PAGE and transferring, the blot was immunolabeled with anti-HA, then stripped and re-probed with anti-UCH-L1. HA blot shows the mono-ubiquitinated UCH-L1 (top panel). C90S mutant form of UCH-L1 has the highest levels of Ub-UCH-L1. Superimposed blot shows both the non-ubiquitinated and mono-ubiquitinated forms of UCH-L1. The HA blot show the levels of free monomeric ubiquitin that are HA positive (lower panels). Therefore, this pool represents the ubiquitin molecules that were bound to UCH-L1. LDN seems to decrease the amount of Ub binding to UCH-L1. Precipication Buffer, PB, contains: 10mM Sodium Phosphate, pH 7.4, 5mM EDTA, 5mM EGTA, and 100 mM NaCla. Ub-UCH-L1: ubiquitinated-UCH-L1.

Generation of RNA interference against UCH-L1

In 2002, it was initially demonstrated that at a given concentration LDN is specific for UCH-L1. The half of maximal inhibitory concentration, IC_{50}, of LDN was shown to be 0.88μM for UCH-L1 and 25μM for its systemic isoform, UCH-L3 (48). Furthermore, our experiments showed that application of a UCH-L3 specific inhibitor does not lead to similar synaptic structural changes as observed in LDN treated neurons (data not shown). These data suggest that the observed phenotypical changes in synaptic structures are mainly due to specific inhibition of UCH-L1. Therefore, we hypothesized that upon reducing the amount of UCH-L1 in neurons we should expect similar synaptic structural changes as seen in LDN treated neurons. To create such scenario, we decided to design an RNAi system which specifically targets UCH-L1 mRNA and degrades it, leading to a reduction in the level of expressed UCH-L1.

After a literature search, it became apparent that UCH-L1 has never previously been knocked down in rat neurons. Therefore, we had to take a trial and error approach in finding the right target sequence within the Uch-l1 gene which could lead to sufficient knockdown. After generating and testing multiple different RNAi constructs against UCH-L1, we eventually came across one that resulted in sufficient knock down of UCH-L1. The target sequence was cloned into p*Silencer™* 1.0-U6 siRNA

expression vector (figure 14). Once the RNAi is transcribed in cells, because of the large complementary region within the resultant mRNA, a hairpin loop structure is generated. This hairpin structure is subsequently cleaved to generate a dsRNA which binds to RISC, RNA-Induced Silencing Complex, and is later melted, generating a 21 base pare single-stranded RNA which remains attached to RISC. If present, the mRNA on the RISC complex specifically hybridizes to a corresponding complimentary region on UCH-L1 mRNAs in the cell. Once bound, the RISC complex cleaves the UCH-L1 mRNA and therefore prevents its translation into UCH-L1 proteins.

Because the specificity of the RISC complex toward its target protein is designated by the mRNA hybridization to the target protein's mRNA, the exact sequence of the mRNA is of special importance for efficient hybridization and knockdown. The target sequence in our designed RNAi is specific for rat UCH-L1, 5'-GGA TGG ATC AGT TCT GAA A-3'; base pairs 327-345 in the rattus UCH-L1 cDNA. Therefore, the designed RNAi was initially tested in C6 rat glial cell line. Since *pSilencer™* 1.0-U6 vector lacks any expression marker, *C6* cells were co-transfected with RNAi and a GFP expressing vector in a 5:1 ratio, respectively. For the control, empty p*Silencer™* vector was co-transfected with the same GFP containing vector in a 5:1 ratio as well. After transfection, C6 cells were allowed to express the RNAi for 3 to 5 days before the amount of UCH-L1

protein was measured using confocal imaging techniques. Cells were fixed, permeabilized and stained with anti-UCH-L1 antibody (figure 15). The arrowheads point at cells which are transfected with the RNAi. Analysis of the fluorescence intensity revealed about 40% reduction in the amount of UCH-L1 in C6 cells.

We wanted to determine the effect of RNAi mediated UCH-L1 reduction in rat hippocampal neurons and examine to see whether this could lead to synaptic structural changes similar to that of LDN. Therefore we tested the efficiency of the designed RNAi in rat hippocampal neurons. Seven to ten days old neurons were co-transfected with either empty p*Silencer™* vector and GFP or the RNAi and a GFP containing vector. RNAi was allowed to be expressed for seven days in these neurons before the cells were fixed, permeabilized and stained with anti-UCH-L1 antibody (figure 16). When comparing the UCH-L1 signal in the RNAi transfected and control transfected, it can be seen that UCH-L1 immuno-fluorescence is reduced dramatically. The arrowhead points at where UCH-L1 staining would have been expected for the green neurons, however, UCH-L1 staining is very dim due to the protein reduction. UCH-L1 fluorescent was measured in control and RNAi transfected neurons for both the entire neuronal cell body (figure 16B) and in dendrites only

(figure 16C). In both cases RNAi was able to successfully reduce the amount of UCH-L1 about 80%.

Figure 14: Transcription of the p*Silencer*™ 1.0-U6 siRNA expression vector to hairpin RNA, processed to functional siRNA.

Forward primer 5'- GGATGGATCAGTTCTGAAATTCAAGAGATTTC-AGAACTGATCCAT CCTTTTTT– 3', reverse primer 5'-AATTAAAAA-AGGATGGATCAGTTCTGAAATCTCTTGAATTTCAGAACTGATCCATCCGGC C – 3' were purchased from Valuegene, annealed, and cloned into p*Silencer*™ expression vector. This construct was then used to confirm UCH-L1 knockdown in C6 rat glial cells and rat hippocampal neurons.

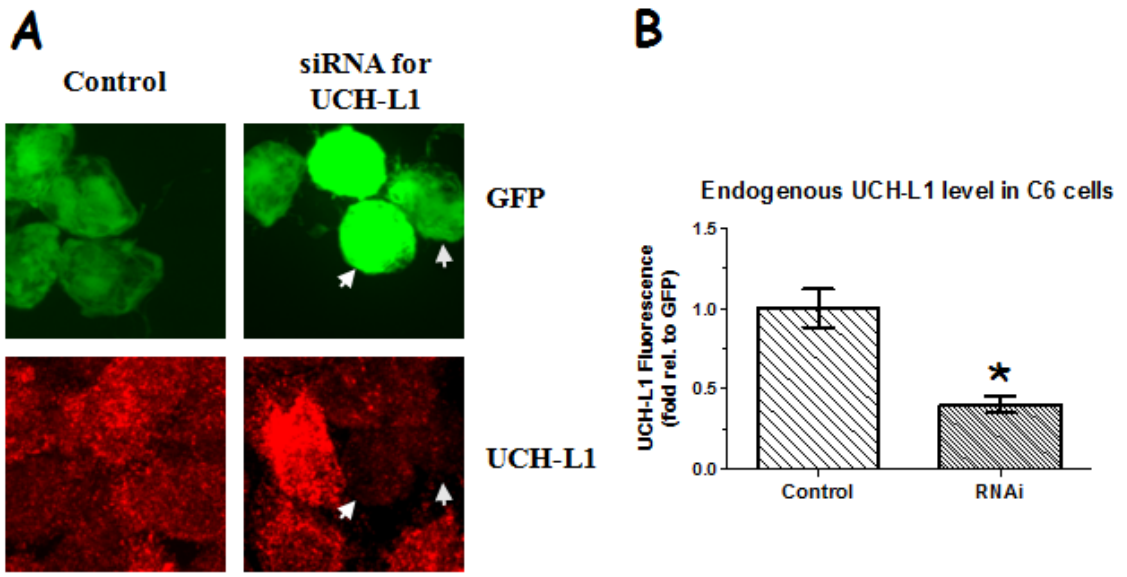

Figure 15: RNAi against UCH-L1 reduces the expression of endogenous UCH-L1 in rat glial C6 cells.

C6 cells were co-transfected with the designed RNAi against UCH-L1and pBOS-GFP for 3-5 days. The RNAi expressing vector p*Silencer™* 1.0-U6 does not contain a GFP protein. Therefore, a molar ratio of 1:5 (pBOS-GFP: RNAi) was used to indentify transfected cells for imaging purposes. ***A***, Representative maximum z-projected confocal images of transfected HEK 293T cells. For control, cells were transfected with pBOS-GFP and empty p*Silencer™* vector (1:5 ration, respectively). Arrows in the lower right panel, are cells that are transfected with the RNAi and have reduced UCH-L1 expression. ***B***, UCH-L1 fluorescent intensity was analyzed for control and RNAi transfected HEK cells. The quantified data were obtained from three independent experiments in which >100 cells were analyzed. Mean values ± SEM are shown. *p<0.001, unpaired Student's *t* test.

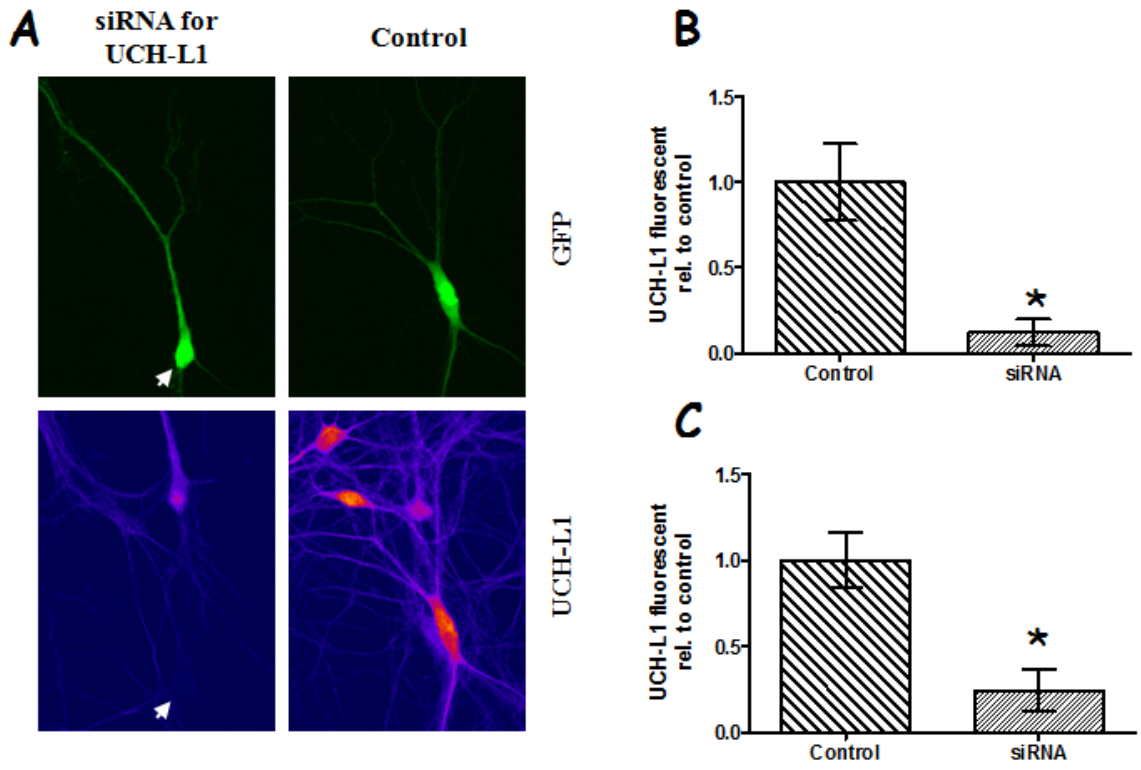

Figure 16: RNAi against UCH-L1 reduces the expression of endogenous UCH-L1 in rat neurons.

Cultured neurons were co-transfected with a molar ratio of 1:5 (pBOS-GFP: empty p*Silencer*™, respectively) as control or co-transfected with pBOS-GFP: *RNAi* (1:5) for 7 days. Then they were fixed, permeabilized, and immunolabeled with anti-UCH-L1. ***A***, Representative maximum z-projected confocal images of transfected neurons. The small arrow in the top left panel points to a green neuron that is positive for RNAi transfection. Indeed, the UCH-L1 staining for that neurons is close to completely gone (lower left panel). Compare this with the UCH-L1 staining for the green cell in the control panels. ***B,C***, UCH-L1 fluorescent was measured in control and RNAi transfected neurons. Both in the entire neuronal cell bodies (***B***) and in dendrites only (***C***) there is a significant decrease in UCH-L1 fluorescent of RNAi transfected cells compared to that of control. Mean values ± SEM are shown. *p<0.01, unpaired Student's *t* test.

RNAi mediated UCH-L1 knock-down does not have the same effect as LDN-57444 on the synaptic protein clusters

To examine whether RNAi mediated UCH-L1 knock-down could lead to similar synaptic structural changes, neurons were transfected with the designed RNAi against UCH-L1. Seven to ten days old cultured neurons were co-transfected with RNAi and GFP, as previously described. After about seven-fourteen days of RNAi expression, neurons were fixed, permeabilized and immunolabeled with anti-UCH-L1 and anti-Shank antibody. Shank is a scaffolding protein seen in post synaptic density. Shank has been shown to be a target of UPS and we previously showed that upon LDN treatment the size of Shank puncta increases dramatically in neurons. In our knock down experiment we stained the neurons with UCH-L1 to confirm once again that UCH-L1 level is reduced. Confocal imaging revealed that even though UCH-L1 was reduced, there was no significant change detected in the size of the Shank protein clusters (figure 17A). Moreover, we analyzed the puncta density as measured by the number of Shank puncta in 10μm of dendrite. Similar to LDN treated neurons which displayed no reduction in the density of Shank puncta, there was also no change in the density of Shank puncta in case of the RNAi mediated knock down(figure 17B). The quantified data represent measurements from more than 50 dendrites for each condition.

Furthermore, we examined if there is any significant effect on other pre-and post-synaptic protein structures when UCH-L1 is knocked down. To do this a similar experiment was preformed but this time the neurons were stained with post-synaptic protein PSD-95 and pre-synaptic protein Synapsin. After 7-14 days of RNAi expression, neurons were analyzed for any changes in synaptic protein clusters (figure 18A). Using image J program, signal for Synapsin punctas were analyzed for any changes in size and density, as previously mentioned (figure 18B). Data revealed no significant difference between control and RNAi transfected neurons. Furthermore, analysis of PSD-95 puncta size and density also did not show any change in size or density when comparing control to RNAi transfected (figure 18C).

Take together, these data might suggest that RNAi mediated knockdown of UCH-L1 does not have the same affect on synaptic protein structure as does the treatment of UCH-L1 inhibitor, LDN. However, a few possible explanations for our observations should be mentioned. As have been previously explained, at a given time, there is only a portion of the UCH-L1 proteins in the cell that are active. Therefore, it is possible that the small portion of UCH-L1 which still gets translated after RNAi transfection is enough for normal function of synapsis. It may be that in order to detect any changes in synaptic structure a higher amount of knockdown is

required. Furthermore, it is possible that given the long duration of our knockdown experiment, a compensation mechanism takes place. Although UCH-L1 is the main DUB in the brain, there are other DUBs which are active in neurons. Their activity might increase in the event of reduction in UCH-L1 levels, preventing any changes in synaptic protein structures.

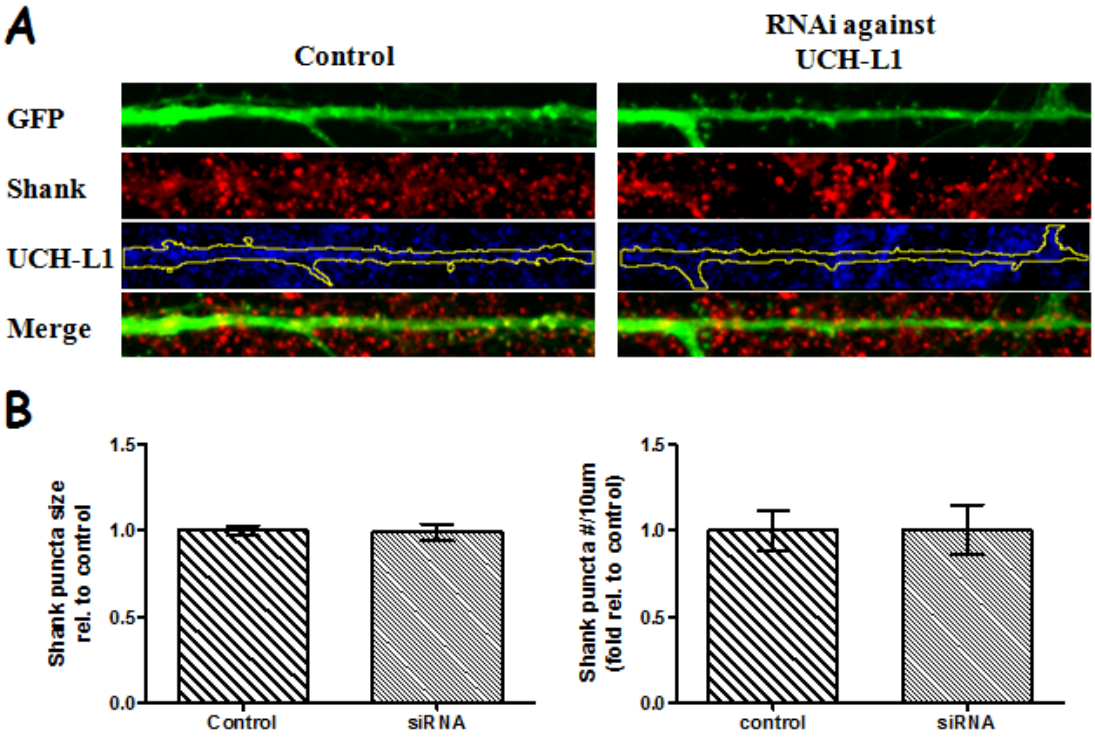

Figure 17: RNAi mediated UCH-L1 knock down has no affect on shank puncta size or number.

Cultured neurons were co-transfected with EGFP alone or EGFP and RNAi, as previously described, for 7-14 days. They were then fixed, permeabilized, and immunolabeled with anti-UCH-L1 and anti-Shank antibodies. ***A***, Representative images of the neurons transfected with control or RNAi constructs. UCH-L1 was successfully reduced, however shank puncta remained the same. The GFP and shank images were superimposed on one another to create the merge. ***B***,***C***, Shank puncta size, ***B***, and number, ***C,*** were analyzed in more than 54 dendrites for each conditions. No significant difference was detected using unpaired Student's *t* test.

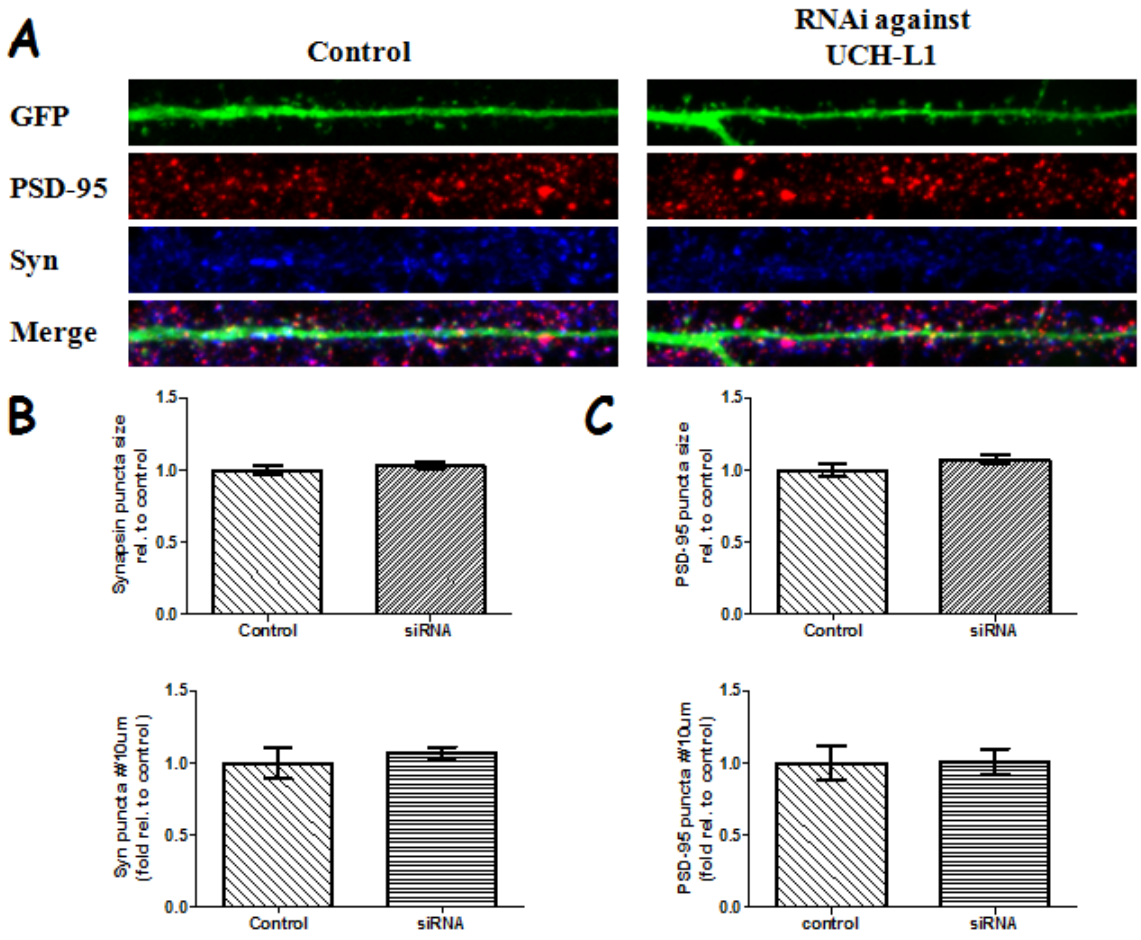

Figure 18: RNAi mediated UCH-L1 knock down has no affect on PSD-95 and Synapsin puncta size or number.

Cultured neurons were co-transfected with EGFP alone or EGFP and RNAi, as previously described, for 7-14 days. Then they were fixed, permeabilized, and immunolabeled with anti-PSD-95 and anti-synapsin antibodies. ***A***, Representative images of the neurons transfected with control or RNAi constructs. Compare the PSD-95 and synapsin puncta. ***B***, Synapsin puncta size, top, and number, bottom, are analyzed. ***C***, PSD-95 puncta size, top, and number, bottom, are analyzed. In both (***B*** and ***C***) more than 30 dendrites were analyzed for each conditions. No significant difference was detected using unpaired Student's *t* test.

Generation of additional tools to study the function of UCH-L1

Aside from RNAi mediated knockdown, over expression studies can be useful in studying UCH-L1 function as well. By creating a dominant negative scenario we can examine how these mutants, some of which have been directly related to diseases, can affect the normal activity of neurons. To be able to perform such experiments, I generated HA-UCH-L1^{WT} and HA-UCH-L1^{mutants} fusion proteins which are cloned into pRK5 vector (figure 19). These constructs can be transfected into neurons and after allowing long term expression of the proteins, we can assess whether over expression of these constructs, each of which has its own function, has any detectable effect on the synaptic structures or the normal physiology of neurons.

Figures 2-9, is a reprint of Figures 2, 3, 8, and part of figure 7 as it appears in Anna E. Cartier, Steven N. Djakovic, Afshin Salehi, Scott M. Wilson, Eliezer Masliah, and Gentry N. Patrick, 2009 Regulation of Synaptic Structure by Ubiquitin C-Terminal Hydrolase L1. J Neurosci, 2009. 29(24): p. 7857-68. The author of the thesis was an author of this paper, and conducted some of the experiments resulting in those figures in collaboration with the other authors.

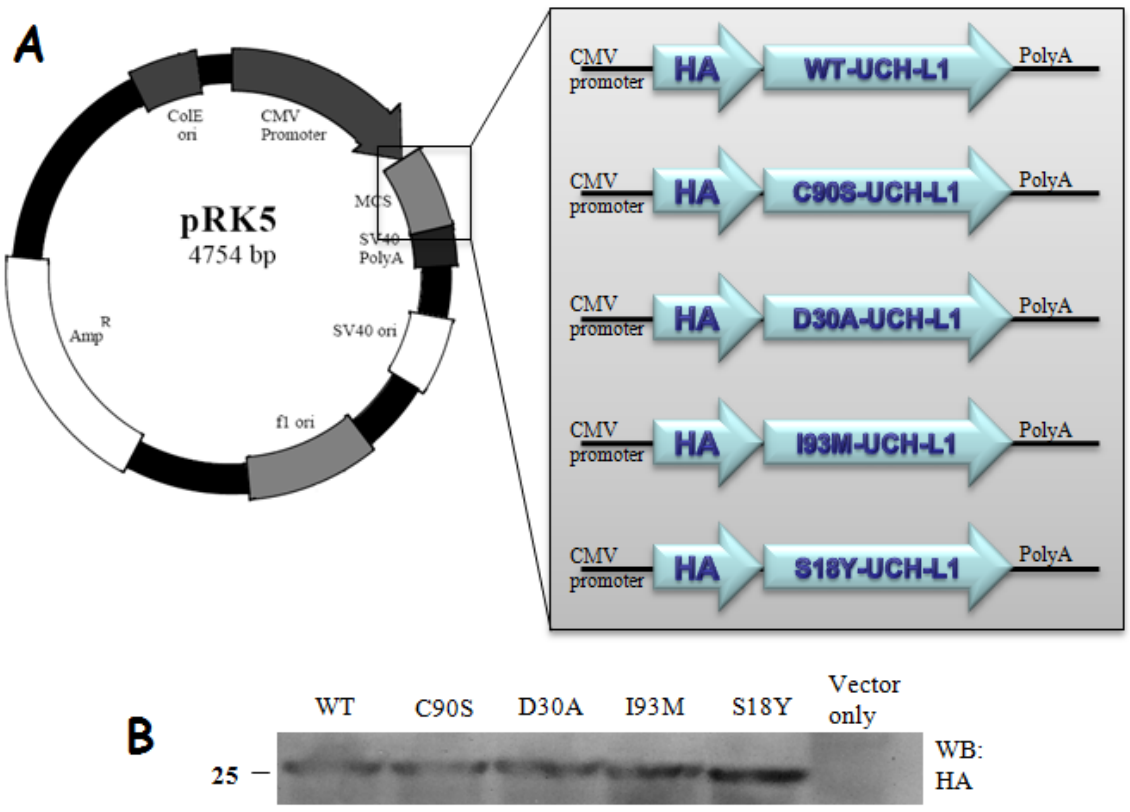

Figure 19: UCH-L1 mutants cloned into pRK5 vector.

Single point mutated forms of UCH-L1 protein which were introduced using PCR-based site-directed mutagenesis were cloned into pRK5 vector (***A***). pRK5 vector contains a CMV promoter that expresses the UCH-L1 at high rate in neurons. HA tag, cloned N-terminus to UCH-L1, can be used to identify transfected cells. To verify the full length expression of the HA-UCH-L1 proteins, HEK 293T cells were transfected and total lysates resolved on SDS-PAGE. Antibody against the HA revealed a distinct band slightly above 25kDa (size of UCH-L1 alone).

DISCUSSION

It is thought that modifications of synaptic efficacy are accompanied by changes in the composition of synaptic proteins. Ubiquitin proteasome system is believed to be an important factor in this remodeling and for synaptic plasticity. However, not much is known about the UPS involvement and their regulation at the synapsis. In the present study, we set out to understand the structure/function of UCH-L1 at the synapsis and to discover any regulatory mechanisms which may exist in neurons to control UCH-L1 function. Furthermore, we studied the effect of a UCH-L1 specific inhibitor, LDN-57444, on the protein function in order to better understand how alteration of UCH-L1 function can lead to changes in synaptic structure.

Using a DUB specific activity probe, which can be utilized to monitor UCH-L1 activity, our data demonstrate that UCH-L1 is partially active in total cell lysates obtained from cultured neurons. Interestingly, we found that 10 minute application of 50μM NMDA/10μM glycine lead to a rapid increase in the activation of UCH-L1. This suggests that UCH-L1 is dynamically regulated by synaptic activity. To determine the specificity of this upregulation of UCH-L1 activity and determine whether it is due to NMDA receptor activation, we applied APV, NMDA receptor antagonist.

Addition of APV at the same time as NMDA, blocked the increase in the activity of UCH-L1, suggesting that the upregulation is at least mainly due to NMDA receptor activation. Concomitant to an increase in UCH-L1 activity, upon NMDA receptor activation, we found that there is also an increase in the level of monomeric ubiquitin in the neurons. This increase in mono-ubiquitin level was blocked when LDN was applied in addition to NMDA receptor agonists. LDN alone resulted in a reduction in mono-Ub levels. Together, these data suggest that UCH-L1 may be responsible for modulating the levels of free monomeric ubiquitin pools available for various cellular processes. Furthermore, it may be that synaptic transmission could be significantly affected by the phenomenon of NMDA-dependant activation of UCH-L1, leading to changes in mono-Ub levels in neurons.

There are many targets of the UPS in the synapses that have been shown to be critical for several forms of synaptic plasticity (6, 76). Since pharmacological inhibition of UCH-L1 has been linked to reduction in LTP (36) and reduced UCH-L1 activity is associated with several neurodegenerative diseases, we wanted to see whether UCH-L1 activity has any effect on synaptic structures. We found that many of the pre- and post-synaptic proteins underwent a rapid redistribution. Particularly, important post synaptic scaffolding proteins Post Synaptic Density-95 (PSD-

95) and Shank experienced this alteration the most. The size of these protein clusters, as well as other synaptic proteins, enlarged by about two folds. Changes in the synaptic protein structures, combined with the LDN effect of reducing mono-ubiquitin levels, suggest a connection between synaptic protein structures and altered monomeric ubiquitin levels in neurons. These alterations in synaptic structures may contribute to the LTP defects observed in UCH-L1 inhibited neurons (36). Strikingly, we were able to show that overexpression of ubiquitin restored normal synaptic structure in LDN-treated neurons. With ubiquitin overexpression in LDN-treated neurons, both the size and the density of the PSD-95 puncta return to that control levels. This further suggests that monomeric ubiquitin level is the underlying reason for changes in synaptic structure upon LDN treatment.

Moreover, using different UCH-L1 mutant forms which exhibit altered functions, we were able to show that while there is no effect on catalytic activity of proteasome, as measured by levels of ubiquitin conjugated proteins, there exists an alteration in the levels of mono-Ub. Strikingly, over-expression of the WT and the C90S forms of UCH-L1, both of which have the ability to bind ubiquitin, resulted in an increase in the levels of mono-Ub in the cells. The D30A mutant form of UCH-L1, which lacks binding ability for ubiquitin and lacks hydrolysis function, was unable to generate the same increase in mono-Ub. These suggest a possible relationship

between UCH-L1 binding ability for ubiquitin, and its ability for hydrolysis, both of which may contribute to alterations in mono-Ub levels in the cell.

Noting that the mutant form D30A, which lacks Ub binding ability, failed to increase ubiquitin levels in the cell, we wanted to see if LDN, also leading to similar results in terms of mono-Ub levels, has any affect on UCH-L1 binding ability. *In vitro* studies using bacterially expressed and purified GST-UCH-L1 which were incubated with pure ubiquitin and LDN show that the binding ability of UCH-L1 for ubiquitin is decreased with a 30 minutes pre-treatment of the protein with its inhibitor, LDN. Furthermore, we show that incubation of UCH-L1 initially with ubiquitin and subsequently adding LDN, also lead to a reduction in the binding ability. These data indicate that aside from LDN's ability to inactivate UCH-L1 hydrolase activity, it is also capable to decreasing UCH-L1 ability to bind Ub. Noting that ubiquitin is degraded through lysosomes and normally through its binding ability UCH-L1 is able to sequester and increase the half life of ubiquitin, it is this combination action of LDN on UCH-L1 which leads to its robust effect of decreases ubiquitin in the cell.

We also tested the effects of LDN on UCH-L1^{WT} and other mutants in *in vivo* studies. While previous studies have shown that WT, I93M, and S18Y mutants are capable of binding ubiquitin (49), we saw that C90S mutant was the only one which was able to maintain binding with ubiquitin even

when using our stringent binding buffer. Along with other components, this buffer contains 1% Trx and 0.1% SDS. This finding suggests that interaction of UCH-L1 with ubiquitin is the strongest in the C90S mutation. However, whether this relatively tightly bound ubiquitin is free to be reused in cells for other UPS mediated process remains to be determined. Moreover, consistent with our *in vitro* experiment, we show that LDN treatment decreases the binding ability of UCH-L1^{C90S} for ubiquitin.

Of another importance, consistent with other studies, we found that UCH-L1 is mono-ubiquitinated in cells (75). The level of mono-ubiquitination displays an interesting pattern among different mutants. Compared to the WT, the C90Smutation showed a higher level of mono-ubiquitination while the D30A mutation displayed less mono-ubiquitination. While another group has suggested an implication between UCH-L1 mono-ubiquitination and UCH-L1 function (75), our data suggests that there may be a link between UCH-L1 binding ability and levels of mono-ubiquitination. D30A which lacks the ability to interact with ubiquitin displays lesser amount of ubiquitination. Contrary to that, the C90S mutation, capable of interacting with ubiquitin is highly mono-ubiquitinated. Furthermore, due to lack of its hydrolase ability it is possible that C90S is not capable of auto-deubiquitinating itself, a previously explained function (75).

In addition to utilizing pharmacological alterations of UCH-L1 function, we also studied UCH-L1 relationship to synaptic protein structural changes using genetic manipulations. For the first time an RNA interference system was designed to knock down UCH-L1 expression in rat hippocampal neurons. Using this novel system we examined effects of UCH-L1 reduction on the structure of synaptic proteins. Multiple pre- and post-synaptic proteins were examined for possible alterations in size and distribution. We show that 60%-80% reduction of UCH-L1 for 7-14 days does not lead to altered synaptic protein structures compared to control samples. However, at this point we cannot conclusively determine that lack of UCH-L1 in neurons does not lead to altered synaptic changes. It is possible that synaptic changes are avoided due to compensation mechanism by other DUBs in the cells. Furthermore, it is possible that higher level of knockdown might be required before any detectable changes occur in synaptic protein clusters.

Other experiments should be performed to further study the effect of UCH-L1 on synaptic protein structural changes. We were able to show that altered synaptic structure seen in LDN treated neurons was concomitant to a reduction in ubiquitin levels in neurons. Therefore, it would be interesting to see whether the RNAi mediated knockdown of UCH-L1 does in fact lead to altered mono-ubiquitin levels in neurons.

Furthermore, it would be informative to examine whether UCH-L1 activity itself is upregulated in case of RNAi mediated knockdown. Such phenomenon could partly explain lack of altered synaptic protein distribution seen in RNAi transfected neurons.

While the presented study opens up many new questions about the structure/function of UCH-L1 in neurons, it does include many novel findings about this brain specific protein which has been linked to many neurodegenerative diseases. We have uncovered a novel link between neuronal activity, UCH-L1 function, the maintenance of fUb levels and regulation of synaptic structures. Furthermore, we uncovered a novel affect of UCH-L1 specific inhibitor LDN on ubiquitin binding ability of this DUB. Lastly, we generated genetic tools to further study the function of UCH-L1 in neurons.

REFERENCES

1. Hicke, L., *Protein regulation by monoubiquitin.* Nat Rev Mol Cell Biol, 2001. **2**(3): p. 195-201.

2. Cardozo, T. and M. Pagano, *The SCF ubiquitin ligase: insights into a molecular machine.* Nat Rev Mol Cell Biol, 2004. **5**(9): p. 739-51.

3. Soligo, D., et al., *The apoptogenic response of human myeloid leukaemia cell lines and of normal and malignant haematopoietic progenitor cells to the proteasome inhibitor PSI.* Br J Haematol, 2001. **113**(1): p. 126-35.

4. Pickart, C.M., *Back to the future with ubiquitin.* Cell, 2004. **116**(2): p. 181-90.

5. Ardley, H.C. and P.A. Robinson, *E3 ubiquitin ligases.* Essays Biochem, 2005. **41**: p. 15-30.

6. Patrick, G.N., *Synapse formation and plasticity: recent insights from the perspective of the ubiquitin proteasome system.* Curr Opin Neurobiol, 2006. **16**(1): p. 90-4.

7. Koegl, M., et al., *A novel ubiquitination factor, E4, is involved in multiubiquitin chain assembly.* Cell, 1999. **96**(5): p. 635-44.

8. Kuhlbrodt, K., J. Mouysset, and T. Hoppe, *Orchestra for assembly and fate of polyubiquitin chains.* Essays Biochem, 2005. **41**: p. 1-14.

9. Yao, T. and R.E. Cohen, *A cryptic protease couples deubiquitination and degradation by the proteasome.* Nature, 2002. **419**(6905): p. 403-7.

10. Song, L. and M. Rape, *Reverse the curse--the role of deubiquitination in cell cycle control.* Curr Opin Cell Biol, 2008. **20**(2): p. 156-63.

11. Daniel, J.A. and P.A. Grant, *Multi-tasking on chromatin with the SAGA coactivator complexes.* Mutat Res, 2007. **618**(1-2): p. 135-48.

12. Guterman, A. and M.H. Glickman, *Deubiquitinating enzymes are IN/(trinsic to proteasome function).* Curr Protein Pept Sci, 2004. **5**(3): p. 201-11.

13. Komada, M., *Controlling receptor downregulation by ubiquitination and deubiquitination.* Curr Drug Discov Technol, 2008. **5**(1): p. 78-84.

14. Schmidt, M., et al., *Proteasome-associated proteins: regulation of a proteolytic machine.* Biol Chem, 2005. **386**(8): p. 725-37.

15. Kennedy, R.D. and A.D. D'Andrea, *The Fanconi Anemia/BRCA pathway: new faces in the crowd.* Genes Dev, 2005. **19**(24): p. 2925-40.

16. Wilkinson, K.D., *Regulation of ubiquitin-dependent processes by deubiquitinating enzymes.* FASEB J, 1997. **11**(14): p. 1245-56.

17. Nijman, S.M., et al., *A genomic and functional inventory of deubiquitinating enzymes.* Cell, 2005. **123**(5): p. 773-86.

18. Baker, R.T. and P.G. Board, *The human ubiquitin gene family: structure of a gene and pseudogenes from the Ub B subfamily.* Nucleic Acids Res, 1987. **15**(2): p. 443-63.

19. Ozkaynak, E., et al., *The yeast ubiquitin genes: a family of natural gene fusions.* EMBO J, 1987. **6**(5): p. 1429-39.

20. Pickart, C.M. and I.A. Rose, *Ubiquitin carboxyl-terminal hydrolase acts on ubiquitin carboxyl-terminal amides.* J Biol Chem, 1985. **260**(13): p. 7903-10.

21. Wilkinson, K.D., et al., *Metabolism of the polyubiquitin degradation signal: structure, mechanism, and role of isopeptidase T.* Biochemistry, 1995. **34**(44): p. 14535-46.

22. Piotrowski, J., et al., *Inhibition of the 26 S proteasome by polyubiquitin chains synthesized to have defined lengths.* J Biol Chem, 1997. **272**(38): p. 23712-21.

23. Liz, M.A. and M.M. Sousa, *Deciphering cryptic proteases.* Cell Mol Life Sci, 2005. **62**(9): p. 989-1002.

24. Bingol, B. and E.M. Schuman, *Synaptic protein degradation by the ubiquitin proteasome system.* Curr Opin Neurobiol, 2005. **15**(5): p. 536-41.

25. Kuo, C.T., et al., *Identification of E2/E3 ubiquitinating enzymes and caspase activity regulating Drosophila sensory neuron dendrite pruning.* Neuron, 2006. **51**(3): p. 283-90.

26. Cohen-Cory, S., *The developing synapse: construction and modulation of synaptic structures and circuits.* Science, 2002. **298**(5594): p. 770-6.

27. Hegde, A.N. and A. DiAntonio, *Ubiquitin and the synapse.* Nat Rev Neurosci, 2002. **3**(11): p. 854-61.

28. Hegde, A.N., *Ubiquitin-proteasome-mediated local protein degradation and synaptic plasticity.* Prog Neurobiol, 2004. **73**(5): p. 311-57.

29. van Roessel, P., et al., *Independent regulation of synaptic size and activity by the anaphase-promoting complex.* Cell, 2004. **119**(5): p. 707-18.

30. Malinow, R., *AMPA receptor trafficking and long-term potentiation.* Philos Trans R Soc Lond B Biol Sci, 2003. **358**(1432): p. 707-14.

31. Hegde, A.N., A.L. Goldberg, and J.H. Schwartz, *Regulatory subunits of cAMP-dependent protein kinases are degraded after conjugation to ubiquitin: a molecular mechanism underlying long-term synaptic plasticity.* Proc Natl Acad Sci U S A, 1993. **90**(16): p. 7436-40.

32. Hou, L., et al., *Dynamic translational and proteasomal regulation of fragile X mental retardation protein controls mGluR-dependent long-term depression.* Neuron, 2006. **51**(4): p. 441-54.

33. Colledge, M., et al., *Ubiquitination regulates PSD-95 degradation and AMPA receptor surface expression.* Neuron, 2003. **40**(3): p. 595-607.

34. Deng, P.Y. and S. Lei, *Long-term depression in identified stellate neurons of juvenile rat entorhinal cortex.* J Neurophysiol, 2007. **97**(1): p. 727-37.

35. Fonseca, R., et al., *A balance of protein synthesis and proteasome-dependent degradation determines the maintenance of LTP.* Neuron, 2006. **52**(2): p. 239-45.

36. Gong, B., et al., *Ubiquitin hydrolase Uch-L1 rescues beta-amyloid-induced decreases in synaptic function and contextual memory.* Cell, 2006. **126**(4): p. 775-88.

37. de Vrij, F.M., et al., *Protein quality control in Alzheimer's disease by the ubiquitin proteasome system.* Prog Neurobiol, 2004. **74**(5): p. 249-70.

38. Upadhya, S.C. and A.N. Hegde, *Ubiquitin-proteasome pathway components as therapeutic targets for CNS maladies.* Curr Pharm Des, 2005. **11**(29): p. 3807-28.

39. Rubinsztein, D.C., *The roles of intracellular protein-degradation pathways in neurodegeneration.* Nature, 2006. **443**(7113): p. 780-6.

40. Chung, K.K., V.L. Dawson, and T.M. Dawson, *The role of the ubiquitin-proteasomal pathway in Parkinson's disease and other neurodegenerative disorders.* Trends Neurosci, 2001. **24**(11 Suppl): p. S7-14.

41. Lowe, J., R.J. Mayer, and M. Landon, *Ubiquitin in neurodegenerative diseases.* Brain Pathol, 1993. **3**(1): p. 55-65.

42. Ross, C.A. and M.A. Poirier, *Protein aggregation and neurodegenerative disease.* Nat Med, 2004. **10 Suppl**: p. S10-7.

43. Anderson, J.P., et al., *Phosphorylation of Ser-129 is the dominant pathological modification of alpha-synuclein in familial and sporadic Lewy body disease.* J Biol Chem, 2006. **281**(40): p. 29739-52.

44. Dahlmann, B., *Role of proteasomes in disease.* BMC Biochem, 2007. **8 Suppl 1**: p. S3.

45. Shimura, H., et al., *Familial Parkinson disease gene product, parkin, is a ubiquitin-protein ligase.* Nat Genet, 2000. **25**(3): p. 302-5.

46. Zhang, Y., et al., *Parkin functions as an E2-dependent ubiquitin-protein ligase and promotes the degradation of the synaptic vesicle-associated protein, CDCrel-1.* Proc Natl Acad Sci U S A, 2000. **97**(24): p. 13354-9.

47. Von Coelln, R., et al., *Loss of locus coeruleus neurons and reduced startle in parkin null mice.* Proc Natl Acad Sci U S A, 2004. **101**(29): p. 10744-9.

48. Liu, Y., et al., *The UCH-L1 gene encodes two opposing enzymatic activities that affect alpha-synuclein degradation and Parkinson's disease susceptibility.* Cell, 2002. **111**(2): p. 209-18.

49. Osaka, H., et al., *Ubiquitin carboxy-terminal hydrolase L1 binds to and stabilizes monoubiquitin in neuron.* Hum Mol Genet, 2003. **12**(16): p. 1945-58.

50. Pankratz, N. and T. Foroud, *Genetics of Parkinson disease.* Genet Med, 2007. **9**(12): p. 801-11.

51. Saigoh, K., et al., *Intragenic deletion in the gene encoding ubiquitin carboxy-terminal hydrolase in gad mice.* Nat Genet, 1999. **23**(1): p. 47-51.

52. Ichihara, N., et al., *Axonal degeneration promotes abnormal accumulation of amyloid beta-protein in ascending gracile tract of gracile axonal dystrophy (GAD) mouse.* Brain Res, 1995. **695**(2): p. 173-8.

53. Case, A. and R.L. Stein, *Mechanistic studies of ubiquitin C-terminal hydrolase L1.* Biochemistry, 2006. **45**(7): p. 2443-52.

54. Wilkinson, K.D., et al., *The neuron-specific protein PGP 9.5 is a ubiquitin carboxyl-terminal hydrolase.* Science, 1989. **246**(4930): p. 670-3.

55. Larsen, C.N., B.A. Krantz, and K.D. Wilkinson, *Substrate specificity of deubiquitinating enzymes: ubiquitin C-terminal hydrolases.* Biochemistry, 1998. **37**(10): p. 3358-68.

56. Finley, D., B. Bartel, and A. Varshavsky, *The tails of ubiquitin precursors are ribosomal proteins whose fusion to ubiquitin facilitates ribosome biogenesis.* Nature, 1989. **338**(6214): p. 394-401.

57. Leroy, E., et al., *The ubiquitin pathway in Parkinson's disease.* Nature, 1998. **395**(6701): p. 451-2.

58. Setsuie, R., et al., *Dopaminergic neuronal loss in transgenic mice expressing the Parkinson's disease-associated UCH-L1 I93M mutant.* Neurochem Int, 2007. **50**(1): p. 119-29.

59. Kahle, P.J., et al., *Subcellular localization of wild-type and Parkinson's disease-associated mutant alpha -synuclein in human and transgenic mouse brain.* J Neurosci, 2000. **20**(17): p. 6365-73.

60. Choi, J., et al., *Oxidative modifications and down-regulation of ubiquitin carboxyl-terminal hydrolase L1 associated with idiopathic Parkinson's and Alzheimer's diseases.* J Biol Chem, 2004. **279**(13): p. 13256-64.

61. Cartier, A.E., et al., *Regulation of synaptic structure by ubiquitin C-terminal hydrolase L1.* J Neurosci, 2009. **29**(24): p. 7857-68.

62. Cho, K.O., C.A. Hunt, and M.B. Kennedy, *The rat brain postsynaptic density fraction contains a homolog of the Drosophila discs-large tumor suppressor protein.* Neuron, 1992. **9**(5): p. 929-42.

63. Carlin, R.K., et al., *Isolation and characterization of postsynaptic densities from various brain regions: enrichment of different types of postsynaptic densities.* J Cell Biol, 1980. **86**(3): p. 831-45.

64. Borodovsky, A., et al., *Chemistry-based functional proteomics reveals novel members of the deubiquitinating enzyme family.* Chem Biol, 2002. **9**(10): p. 1149-59.

65. Sheng, M. and M.J. Kim, *Postsynaptic signaling and plasticity mechanisms.* Science, 2002. **298**(5594): p. 776-80.

66. Sakurai, M., et al., *Reduction in memory in passive avoidance learning, exploratory behaviour and synaptic plasticity in mice with*

a spontaneous deletion in the ubiquitin C-terminal hydrolase L1 gene. Eur J Neurosci, 2008. **27**(3): p. 691-701.

67. Ehlers, M.D., *Activity level controls postsynaptic composition and signaling via the ubiquitin-proteasome system.* Nat Neurosci, 2003. **6**(3): p. 231-42.

68. Lee, S.H., et al., *Synaptic protein degradation underlies destabilization of retrieved fear memory.* Science, 2008. **319**(5867): p. 1253-6.

69. Guo, L. and Y. Wang, *Glutamate stimulates glutamate receptor interacting protein 1 degradation by ubiquitin-proteasome system to regulate surface expression of GluR2.* Neuroscience, 2007. **145**(1): p. 100-9.

70. El-Husseini, A.E., et al., *PSD-95 involvement in maturation of excitatory synapses.* Science, 2000. **290**(5495): p. 1364-8.

71. Murthy, V.N., et al., *Inactivity produces increases in neurotransmitter release and synapse size.* Neuron, 2001. **32**(4): p. 673-82.

72. Johnston, S.C., et al., *Structural basis for the specificity of ubiquitin C-terminal hydrolases.* EMBO J, 1999. **18**(14): p. 3877-87.

73. Sakurai, M., et al., *Ubiquitin C-terminal hydrolase L1 regulates the morphology of neural progenitor cells and modulates their differentiation.* J Cell Sci, 2006. **119**(Pt 1): p. 162-71.

74. Maraganore, D.M., et al., *Case-control study of the ubiquitin carboxy-terminal hydrolase L1 gene in Parkinson's disease.* Neurology, 1999. **53**(8): p. 1858-60.

75. Meray, R.K. and P.T. Lansbury, Jr., *Reversible monoubiquitination regulates the Parkinson disease-associated ubiquitin hydrolase UCH-L1.* J Biol Chem, 2007. **282**(14): p. 10567-75.

76. Yi, J.J. and M.D. Ehlers, *Emerging roles for ubiquitin and protein degradation in neuronal function.* Pharmacol Rev, 2007. **59**(1): p. 14-39.